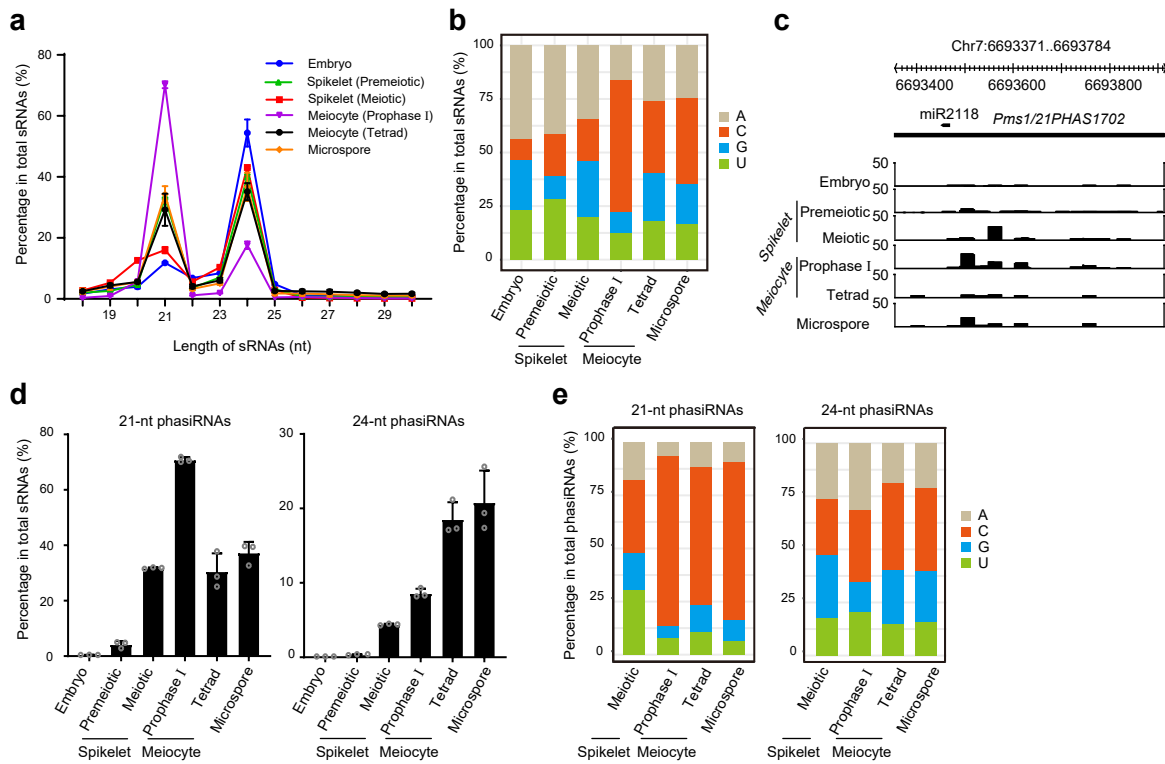
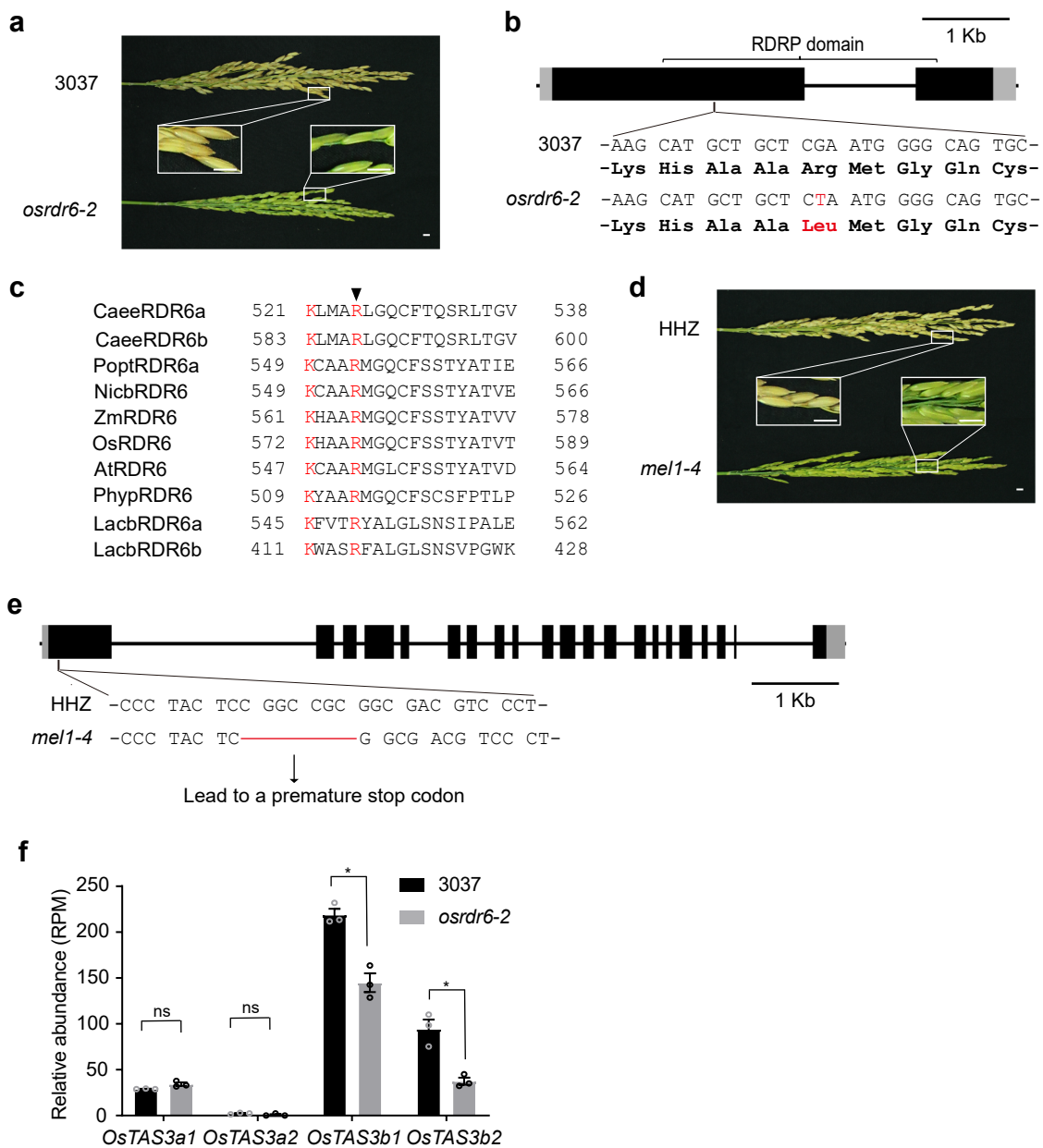


## Supplementary Information

### Supplementary Figures



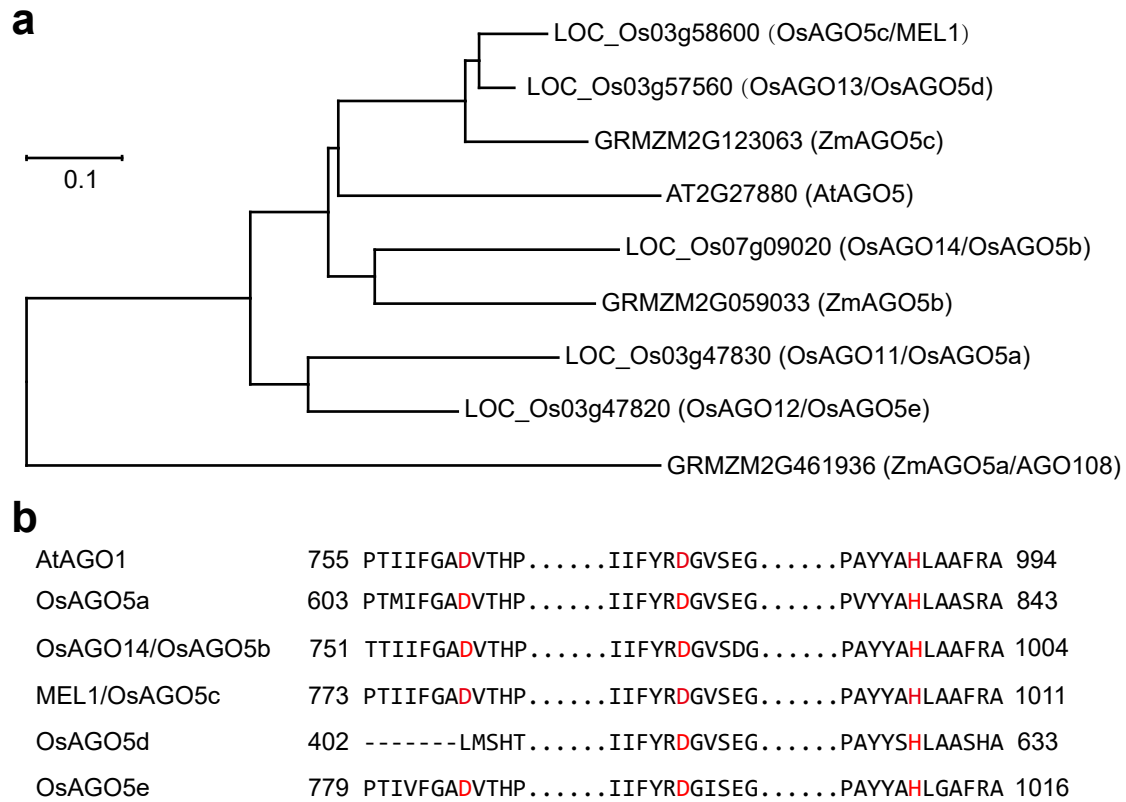
**Supplementary Fig. 1. Profiling of phasiRNAs in rice spikelets and purified germ cells.** **a**, Length distribution of genome-matched sRNAs in embryos, spikelets, meiocytes and microspores. **b**, 5' terminal nucleotide frequency of genome-matched sRNAs in embryos, spikelets, meiocytes and microspores. **c**, Genome browser views of 21-nt phasiRNA signals at the *Pms1* locus in embryos, spikelets, meiocytes and microspores. The y-axis represents sRNA abundance (RPM). **d**, Percentages of 21- and 24-nt phasiRNAs in total genome-matched sRNAs in embryos, spikelets, meiocytes and microspores. The error bars represent standard deviation of three biological replicates. **e**, 5' terminal nucleotide frequency of 21- and 24-nt phasiRNAs in meiotic spikelets, meiocytes and microspores.



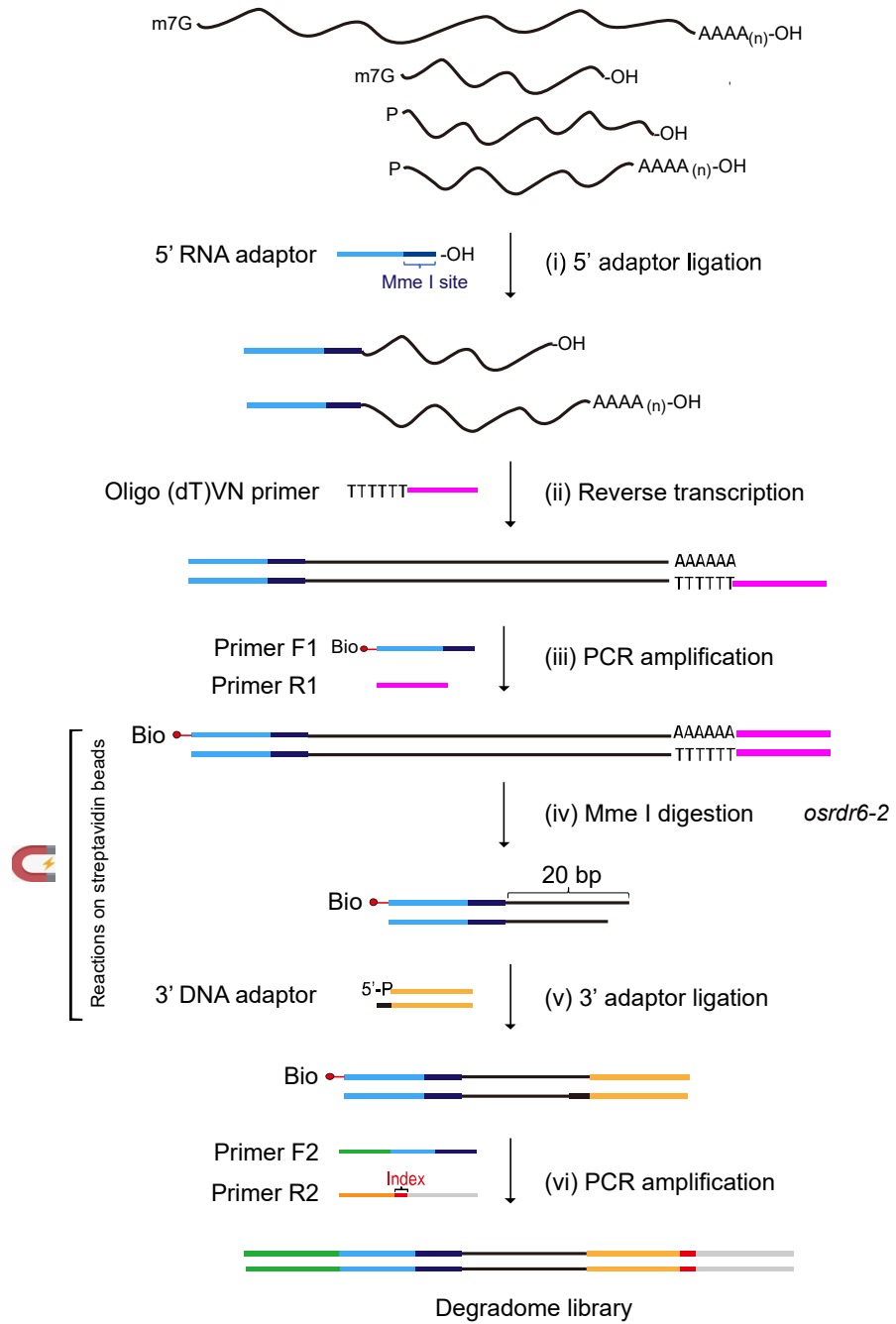
**Supplementary Fig. 2. Characterization of the *osrdr6-2* and *mel1-4* mutants.**

**a**, Panicles of *osrdr6-2* and 3037 rice plants at the grain-filling stage. Note that the seeds of *osrdr6-2* are unfilled and green. Scale bars, 0.5 cm. **b**, Gene structures of *OsRDR6*. Exons are indicated by boxes and introns are indicated by lines. *osrdr6-2* carries point mutation that leads to an amino acid change. **c**, Alignment of partial RDR6 protein sequences. The sequences were aligned with ClustalX. Conserved residues are shown in red. **d**, Panicles of *mel1-4* and HHZ rice plants at the grain-filling stage. Note that the seeds of *mel1-4* are unfilled and green. Scale bars, 0.5 cm. **e**, Gene structures of *MEL1*. Exons are

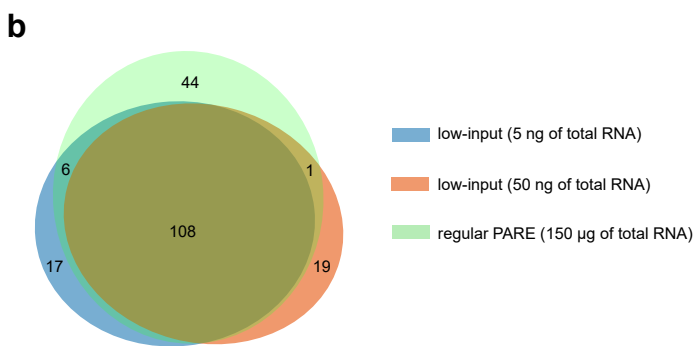
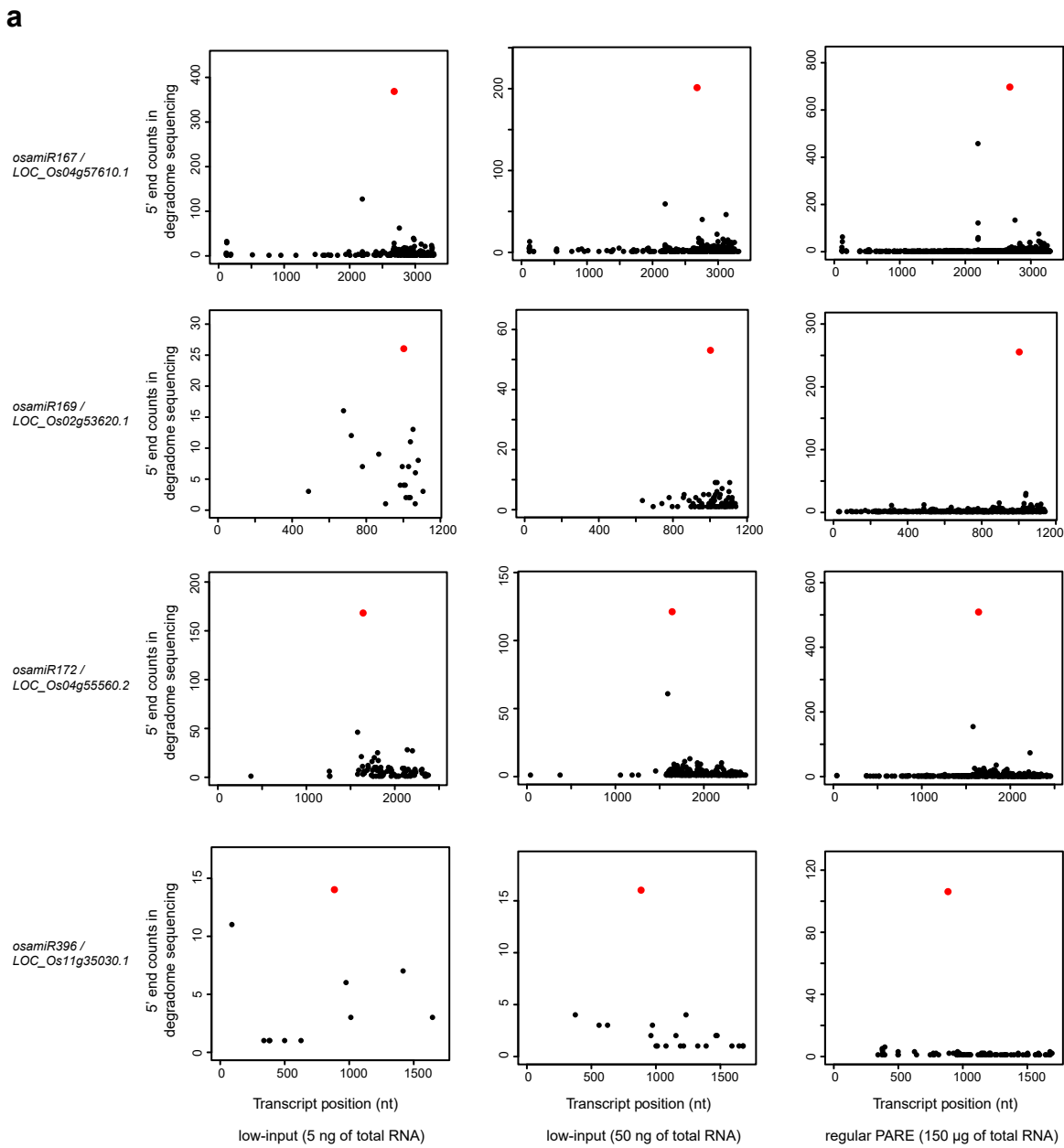
indicated by boxes and introns are indicated by lines. *me1-4* has a deletion mutation that results in a premature stop codon. **f**, Relative accumulation levels of *TAS3*-derived tasiRNAs in early prophase I meiocytes of 3037 and *osrdr6-2*. The error bars represent standard deviation of three biological replicates. Asterisks indicate significant differences between *osrdr6-2* and the corresponding wild-type 3037 plants. \*, Student's t test,  $p$ -value  $\leq 0.05$ .



**Supplementary Fig. 3. AGO5 subclade proteins in rice, maize and *Arabidopsis*.** **a**, Phylogenetic analysis of AGO5 proteins in rice, maize and *Arabidopsis*. The neighbor joining tree was constructed using the MEGAX software. At, *Arabidopsis thaliana*; Os, *Oryza sativa*; Zm, *Zea mays*. Scale bars, 0.1 substitutions per amino acid position. **b**, Alignment of AGO5 protein sequences. The sequences were aligned with ClustalX. Residues forming the catalytic DDH motif are shown in red.

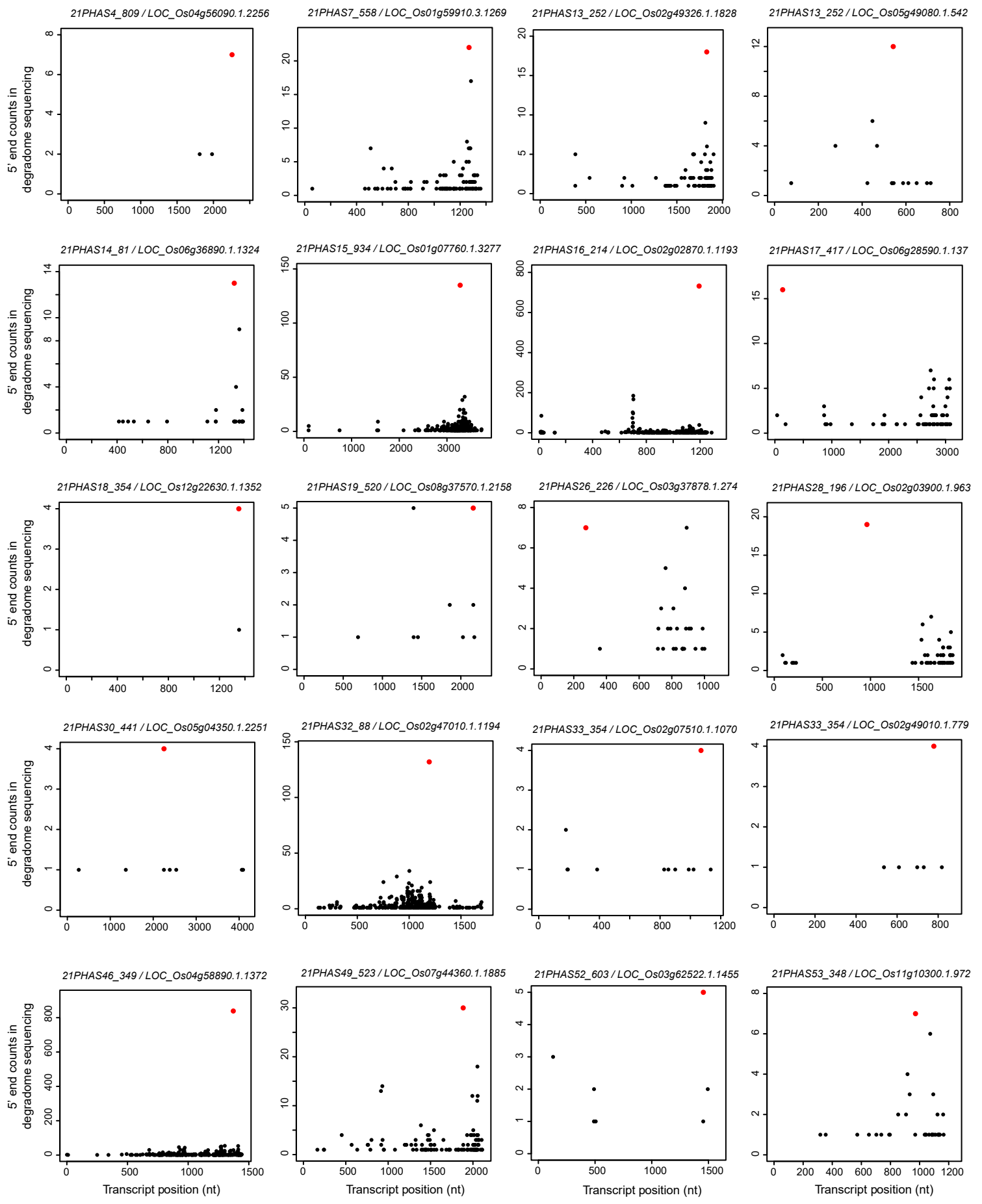


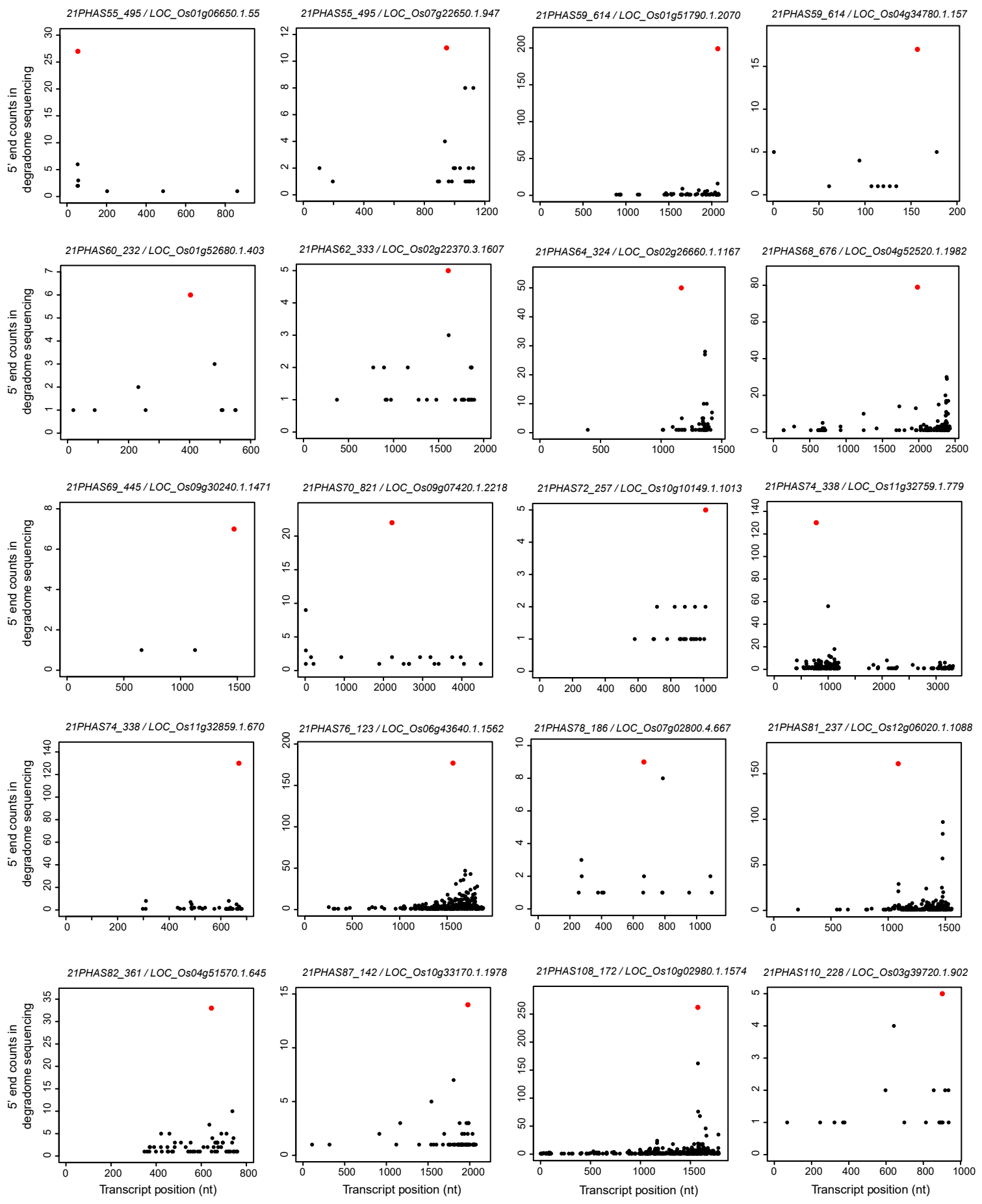
**Supplementary Fig. 4. Schematic depiction of low-input degradome library construction.** Construction of a degradome library for low-input RNAs includes the following steps: (i) RNA with 5'-monophophates group in total RNA is ligated to the 5' RNA adaptor; (ii) the ligated product with 3' poly-A is reverse-transcribed with Oligo-dT<sub>30</sub>VN primer; (iii) the reverse transcription product is purified and amplified with biotin-labelled primer F1 and primer R1; (iv) the PCR product was purified and digested with Mmel; (v) the digested product is purified and ligated to the 3' DNA adaptor; (vi) the final ligated product is purified and amplified with primer F2 and primer R2.

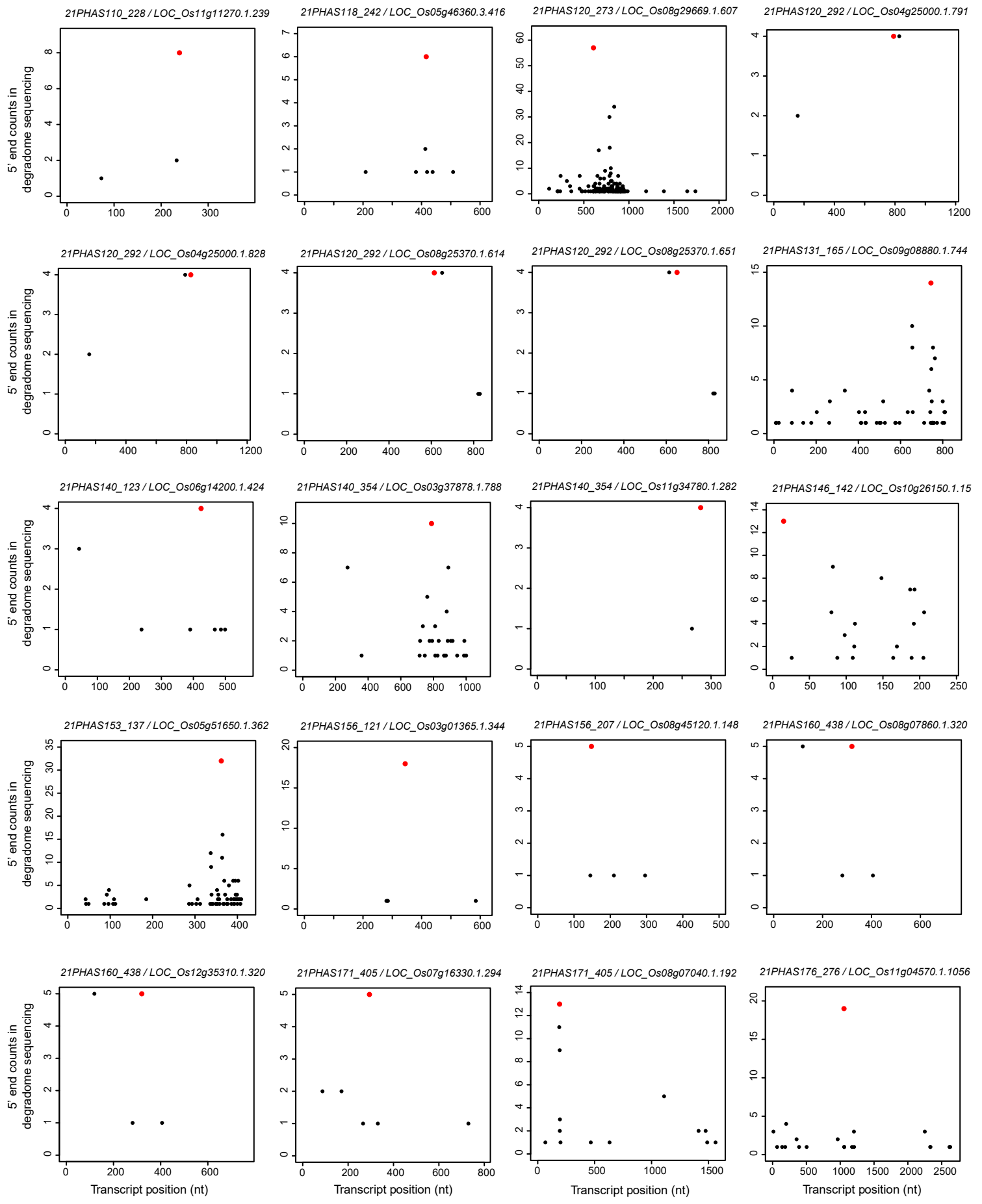


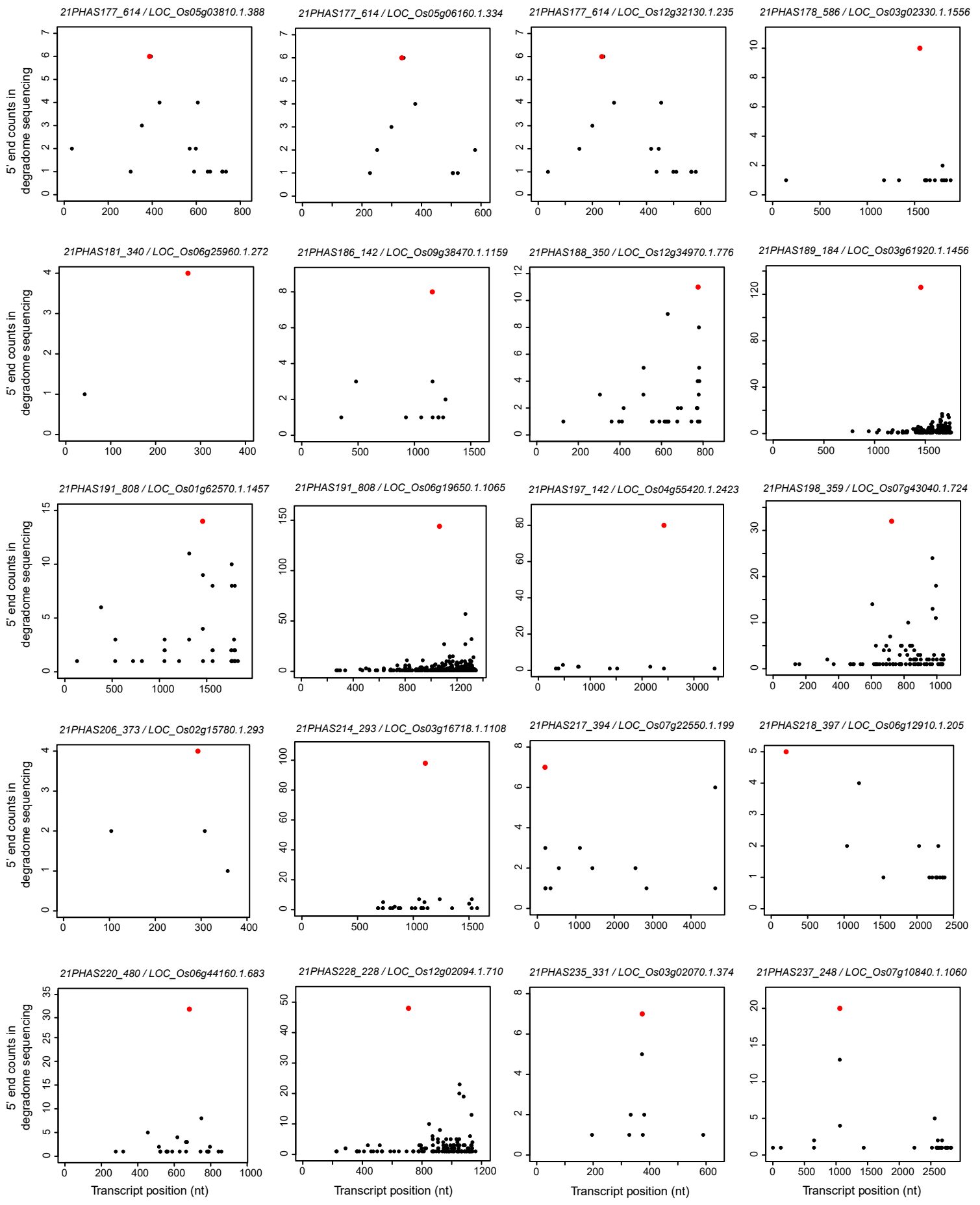
**Supplementary Fig. 5. Comparison of the specificity of the low-input and regular PARE protocols.** **a,** Plots showing the distribution of the degradome tags along miRNA targets. The x-axis represents the nucleotide position of each target mRNA (5'-3'). The y-axis represents the

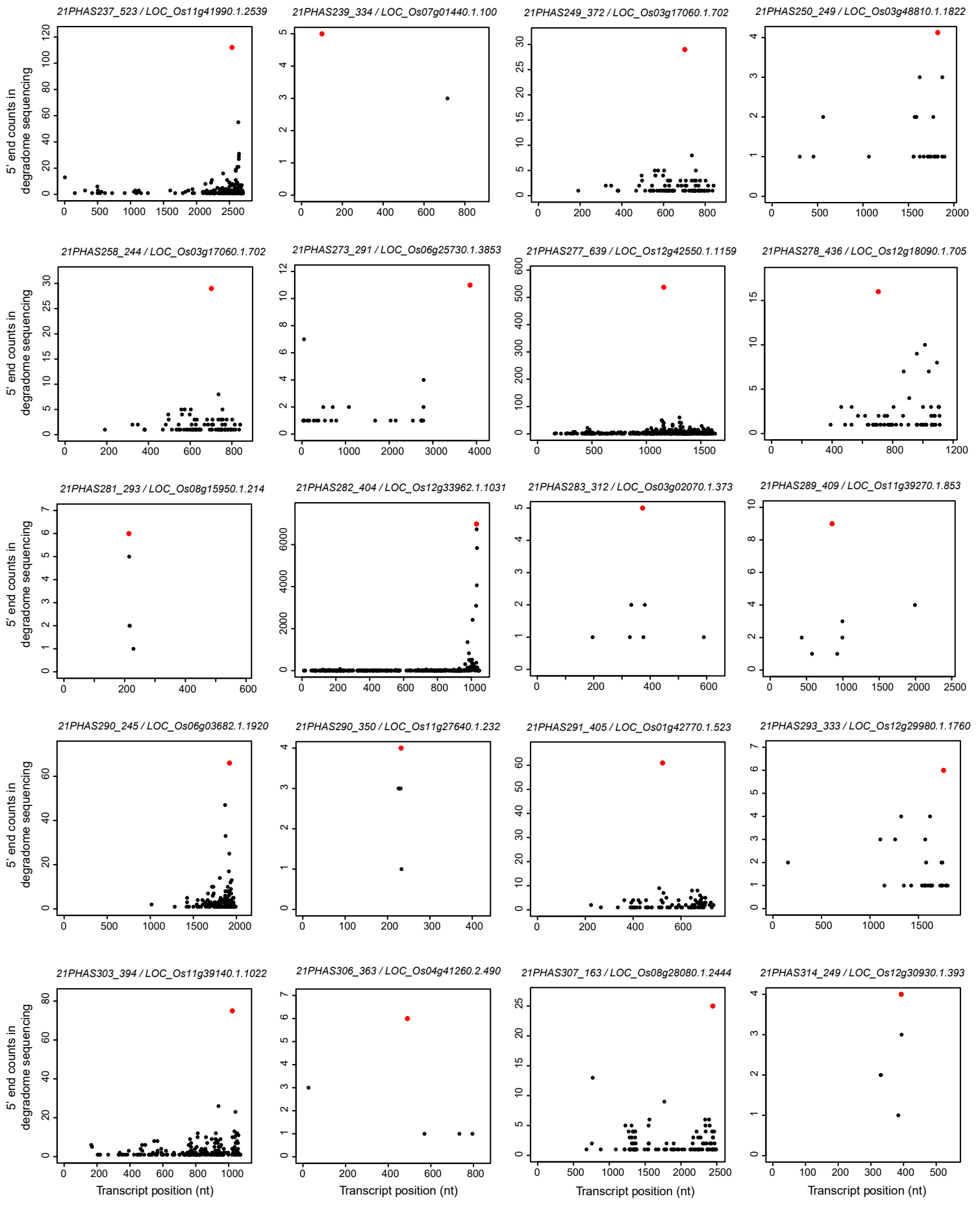
relative frequency of degradome tags. The red dot represents degradome tag at +1 position of miRNA-guided cleavage site. **b**, Venn diagram showing the overlap between miRNA targets identified by the low-input protocol (with 5 ng and 50 ng of total RNA) and the regular PARE protocol (with 150 µg of total RNA).

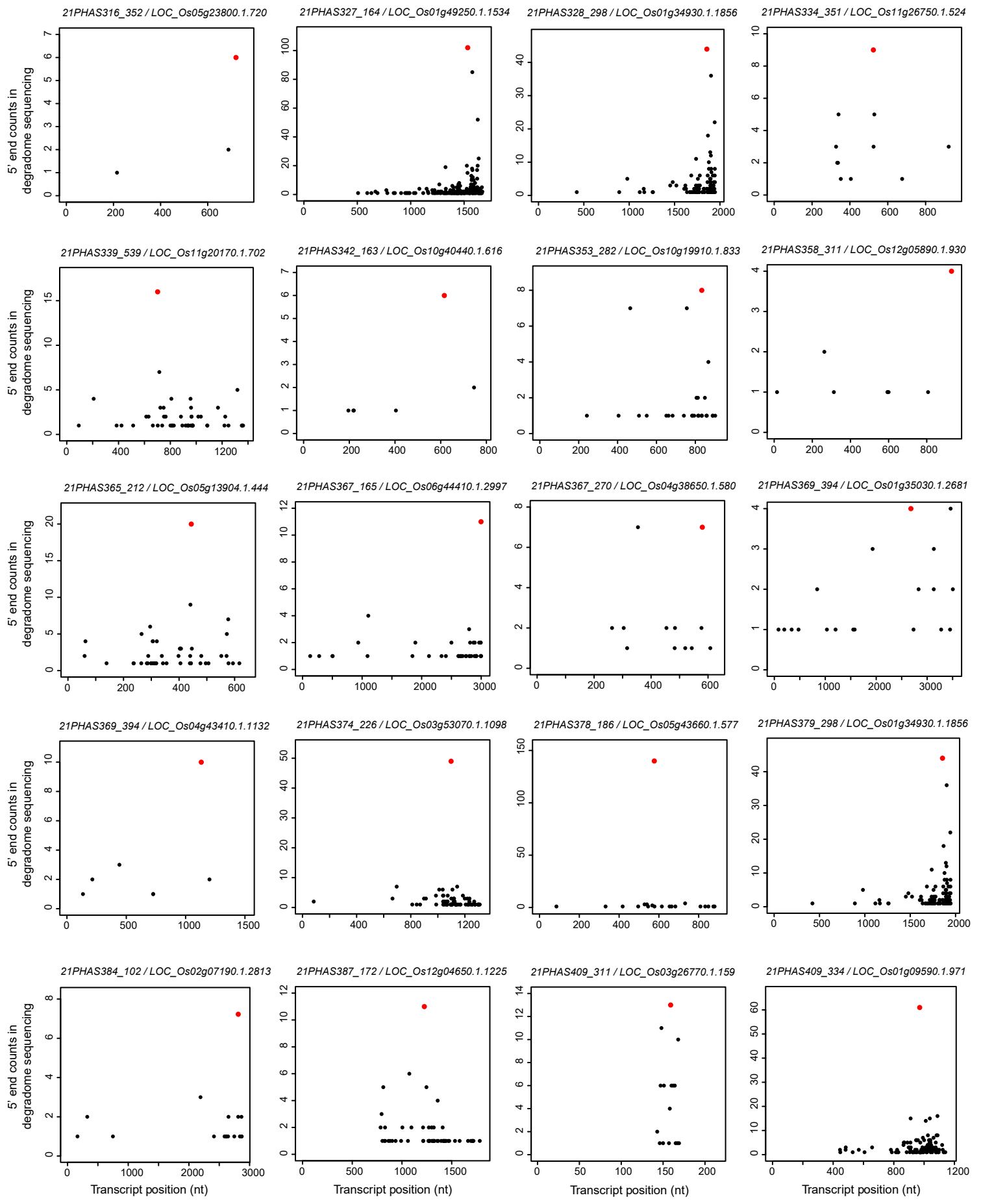


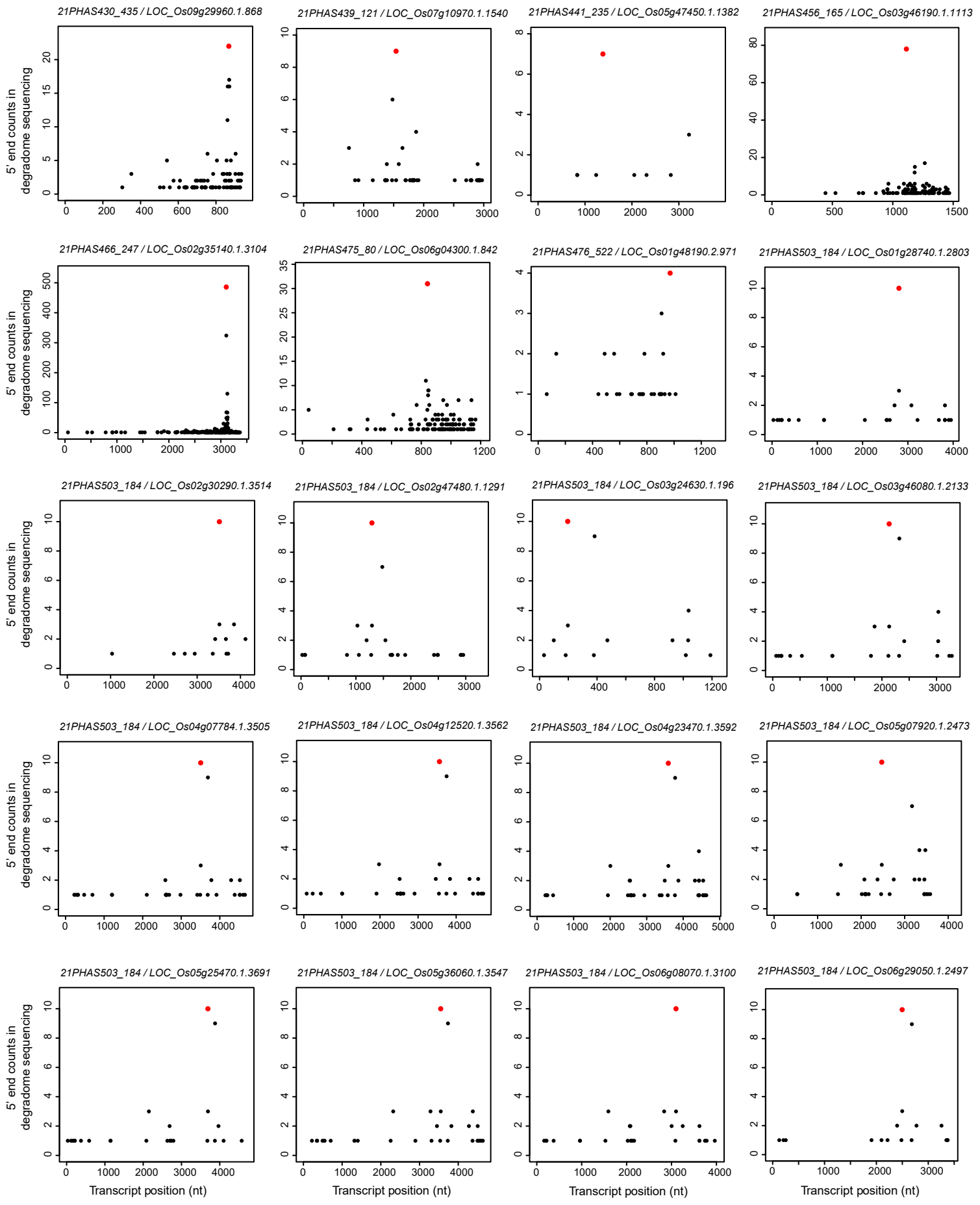


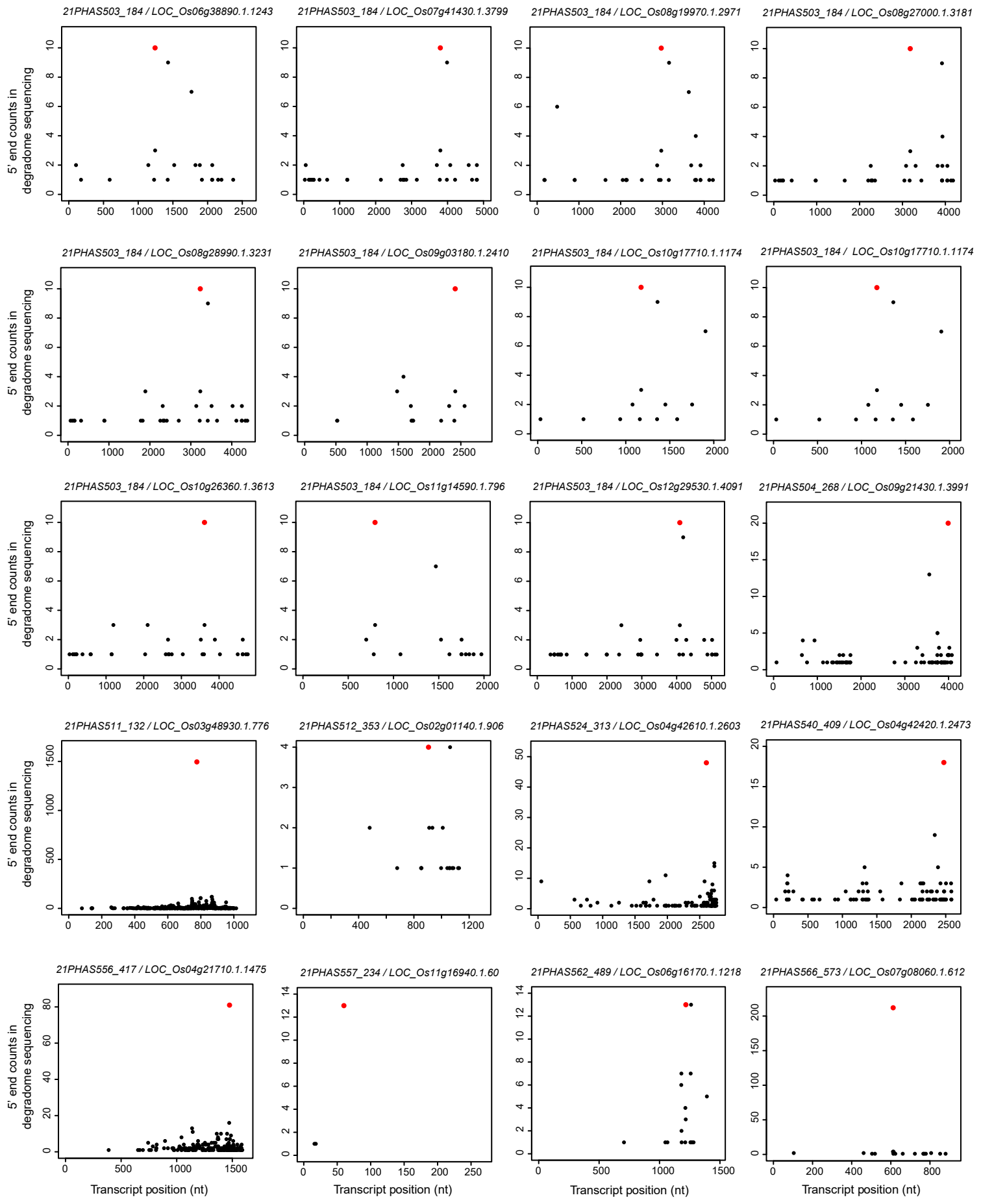


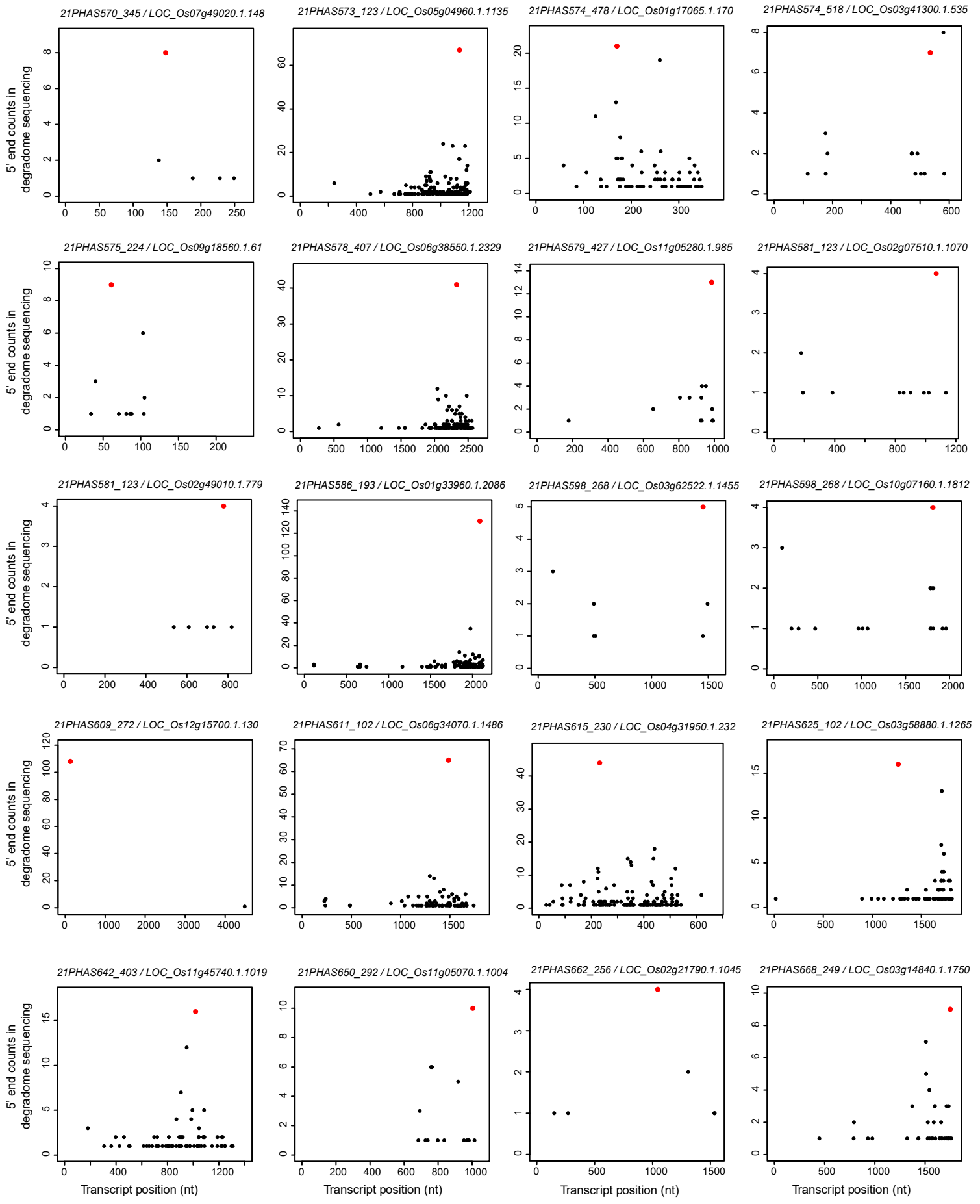


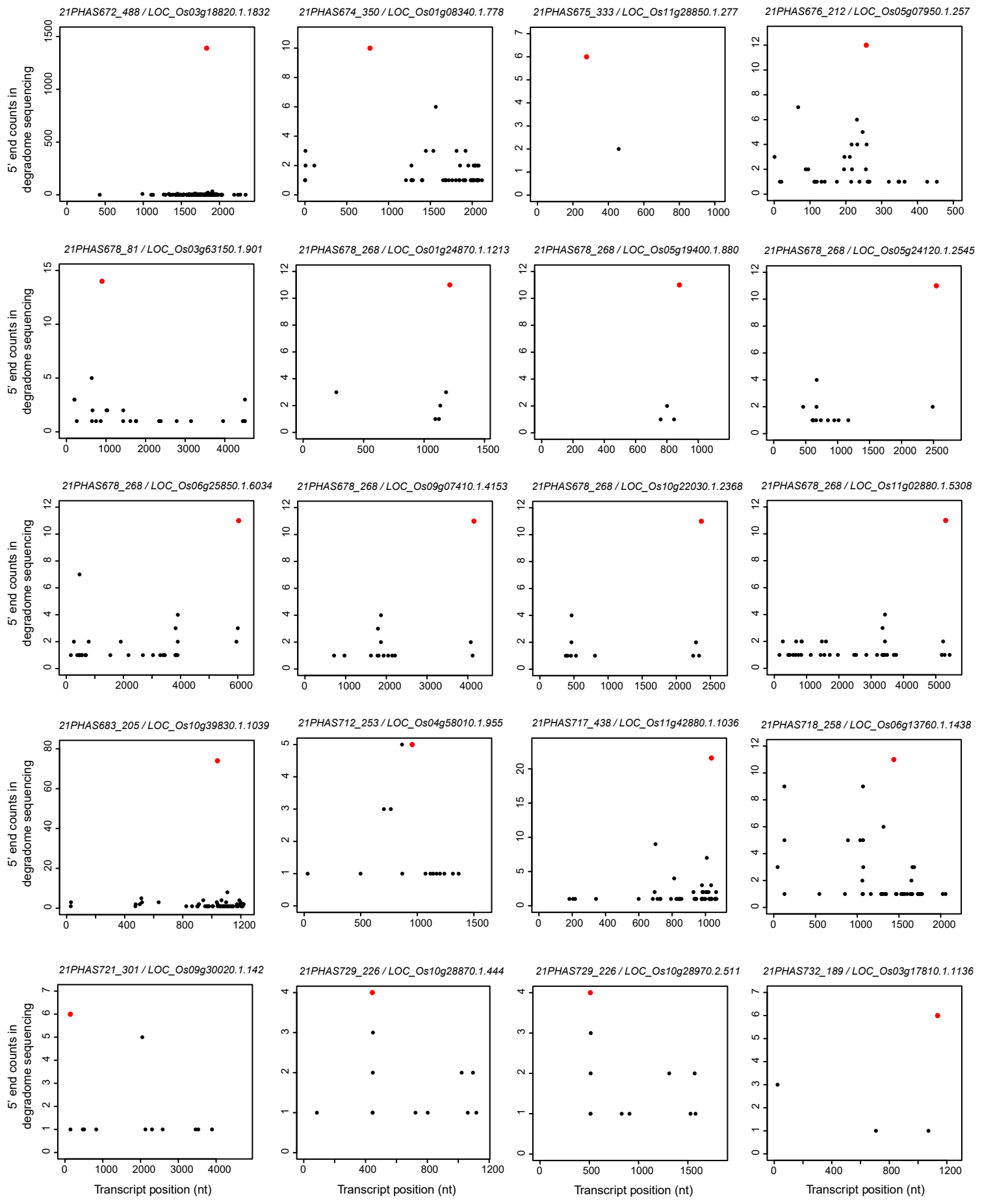


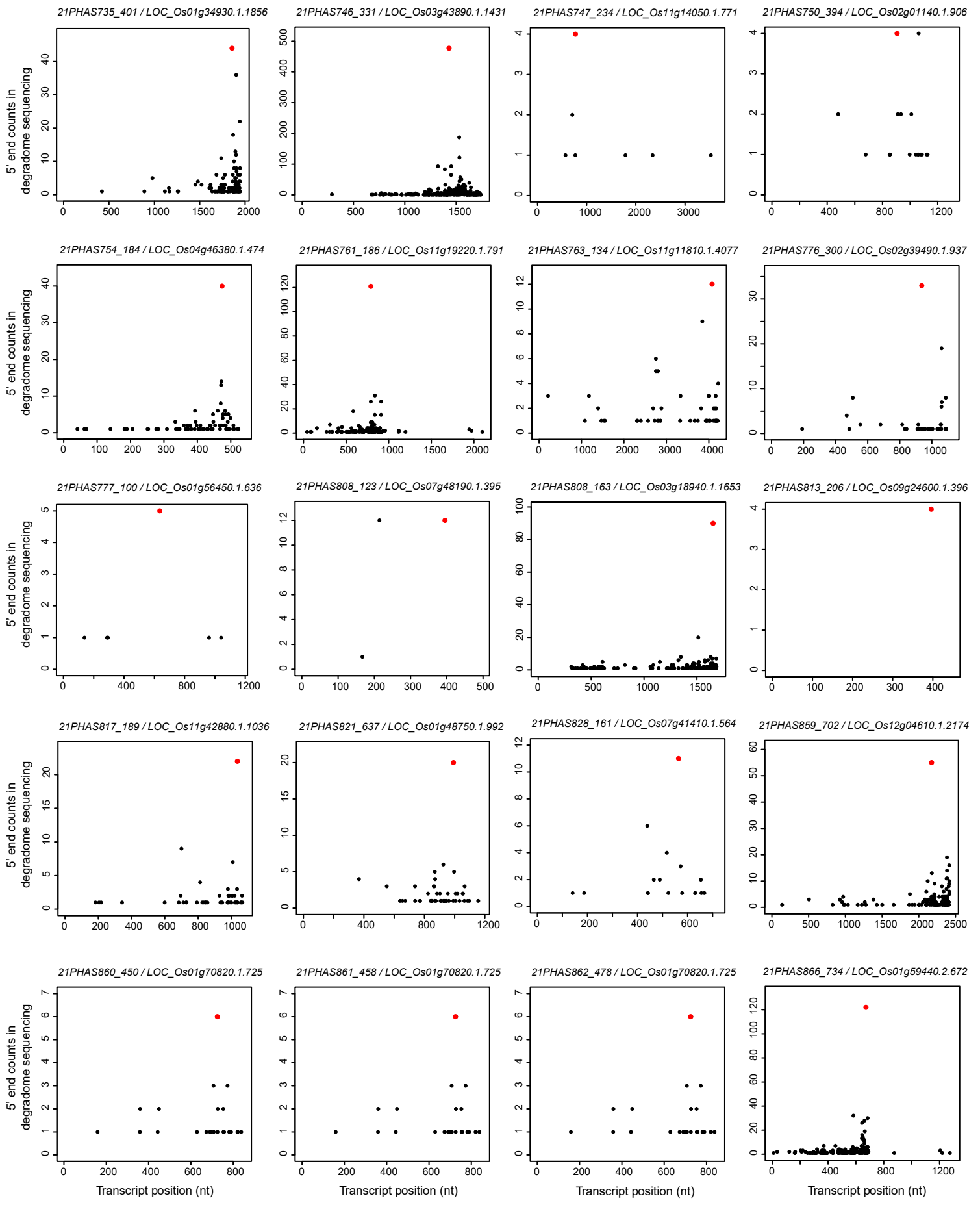


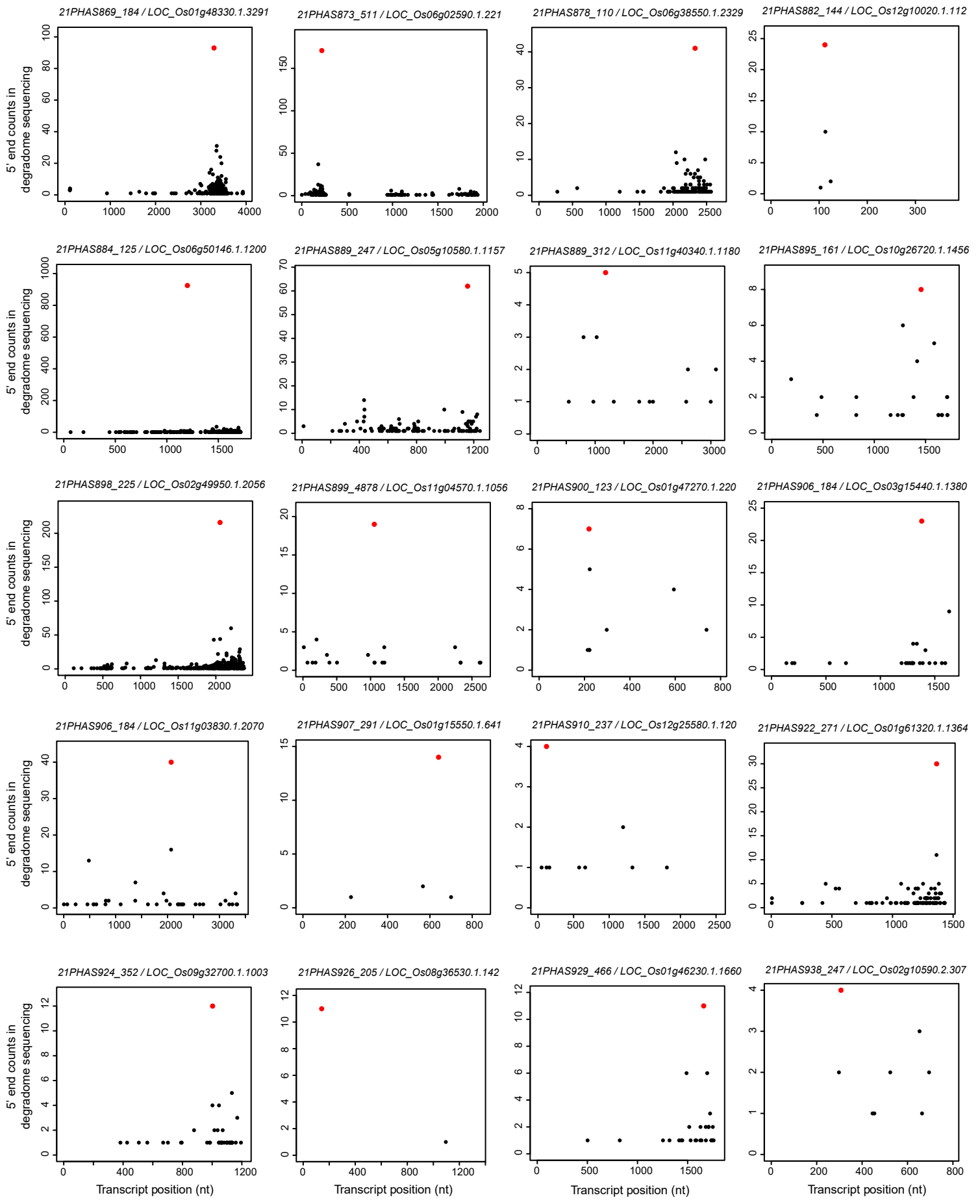


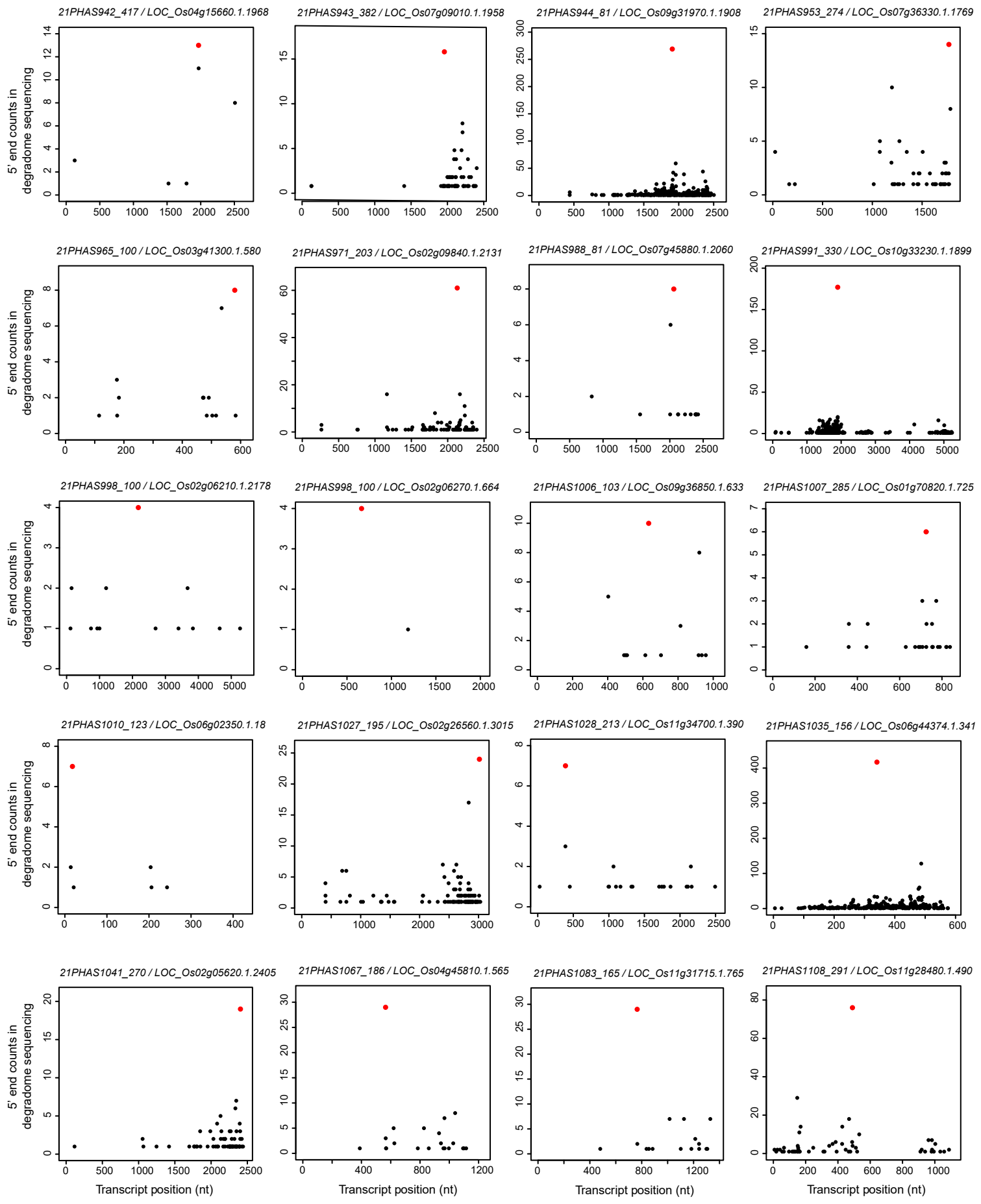


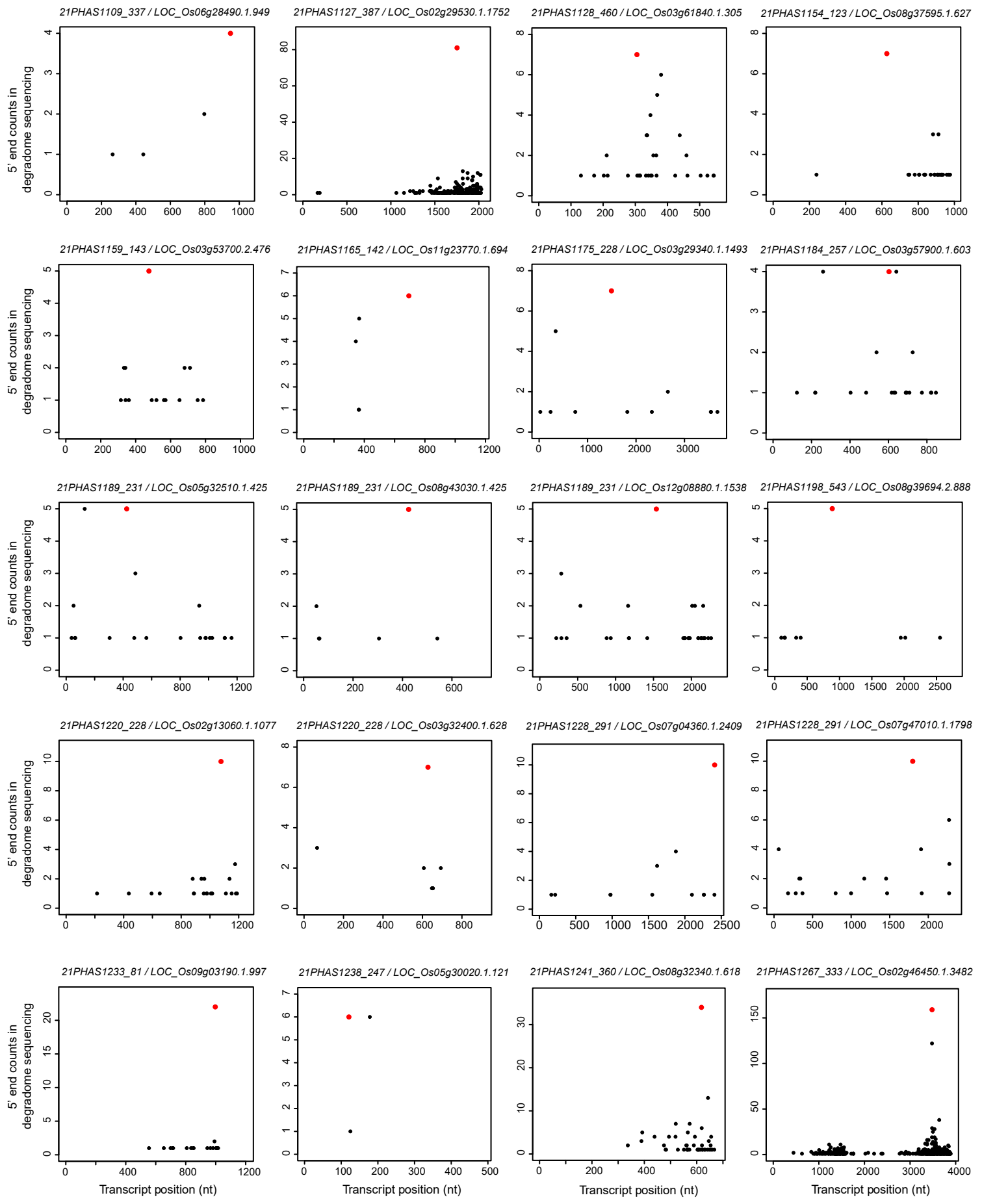


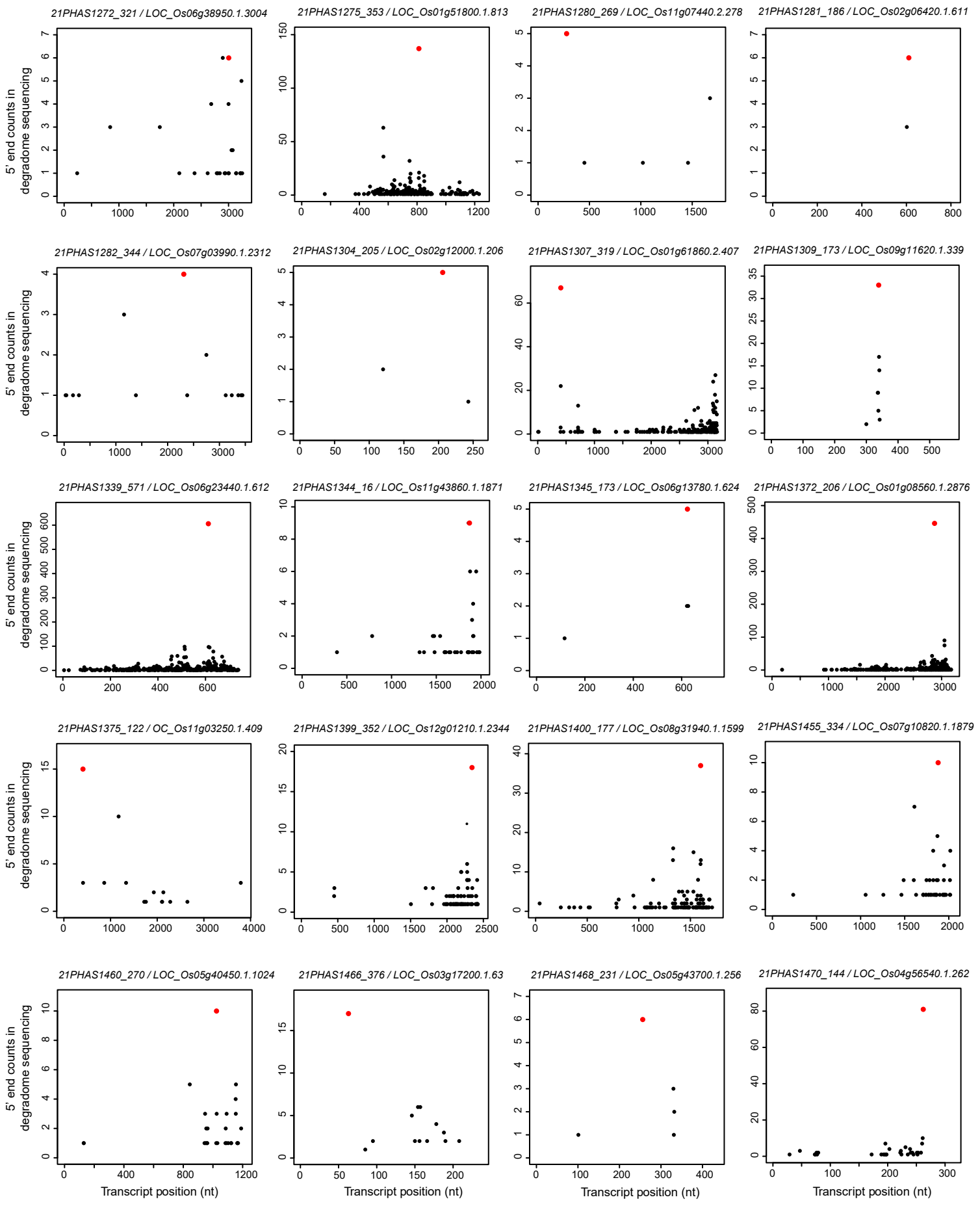


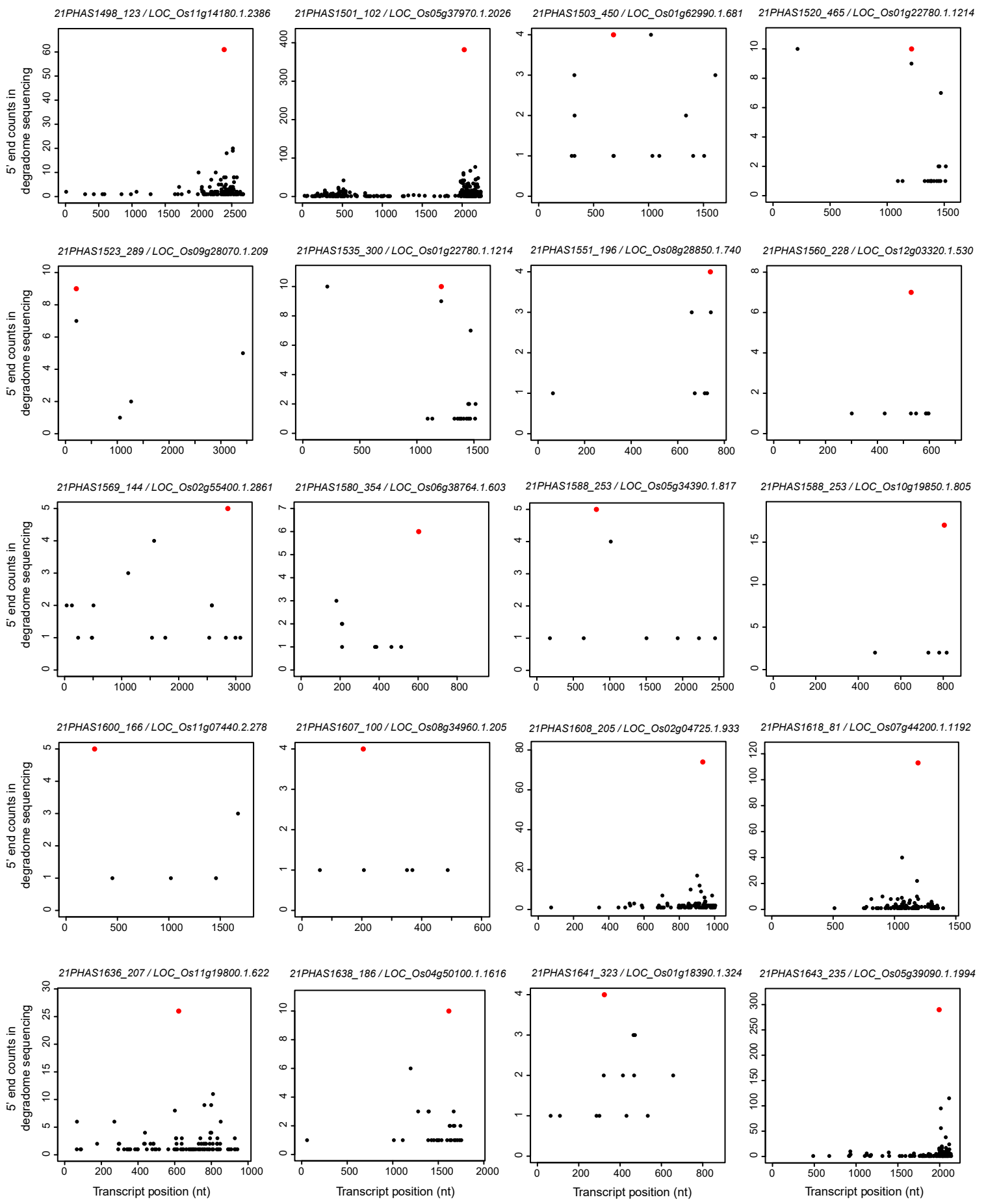


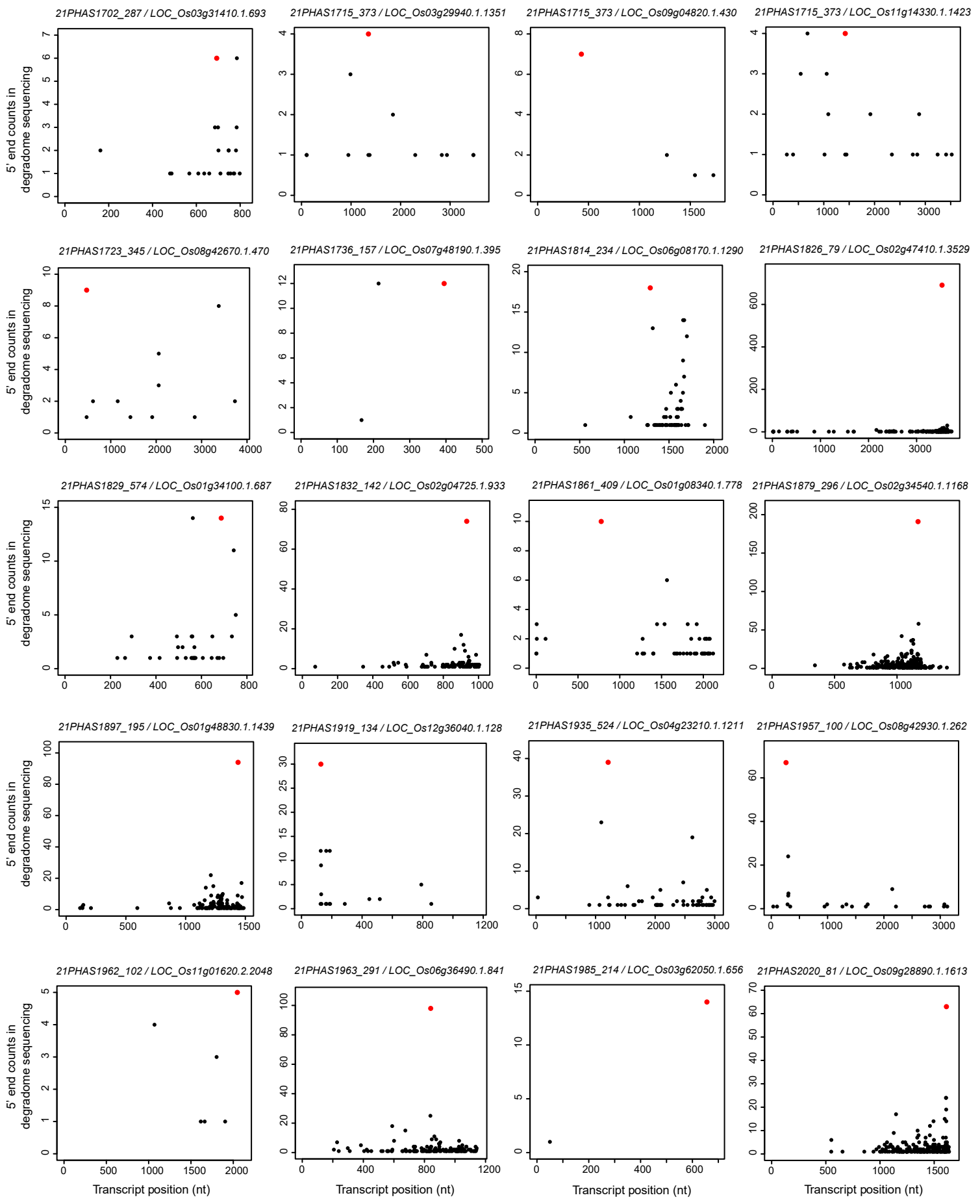


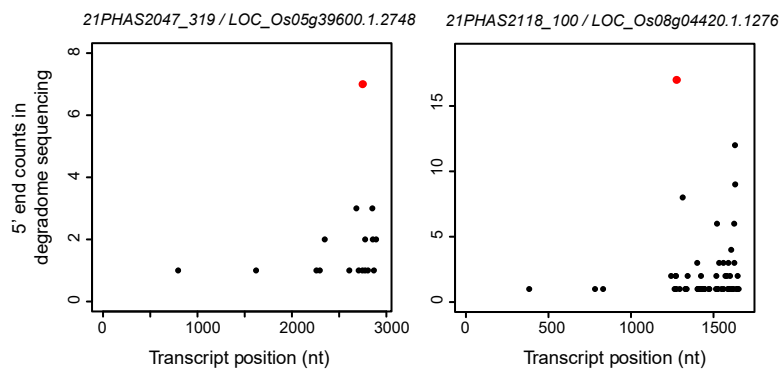




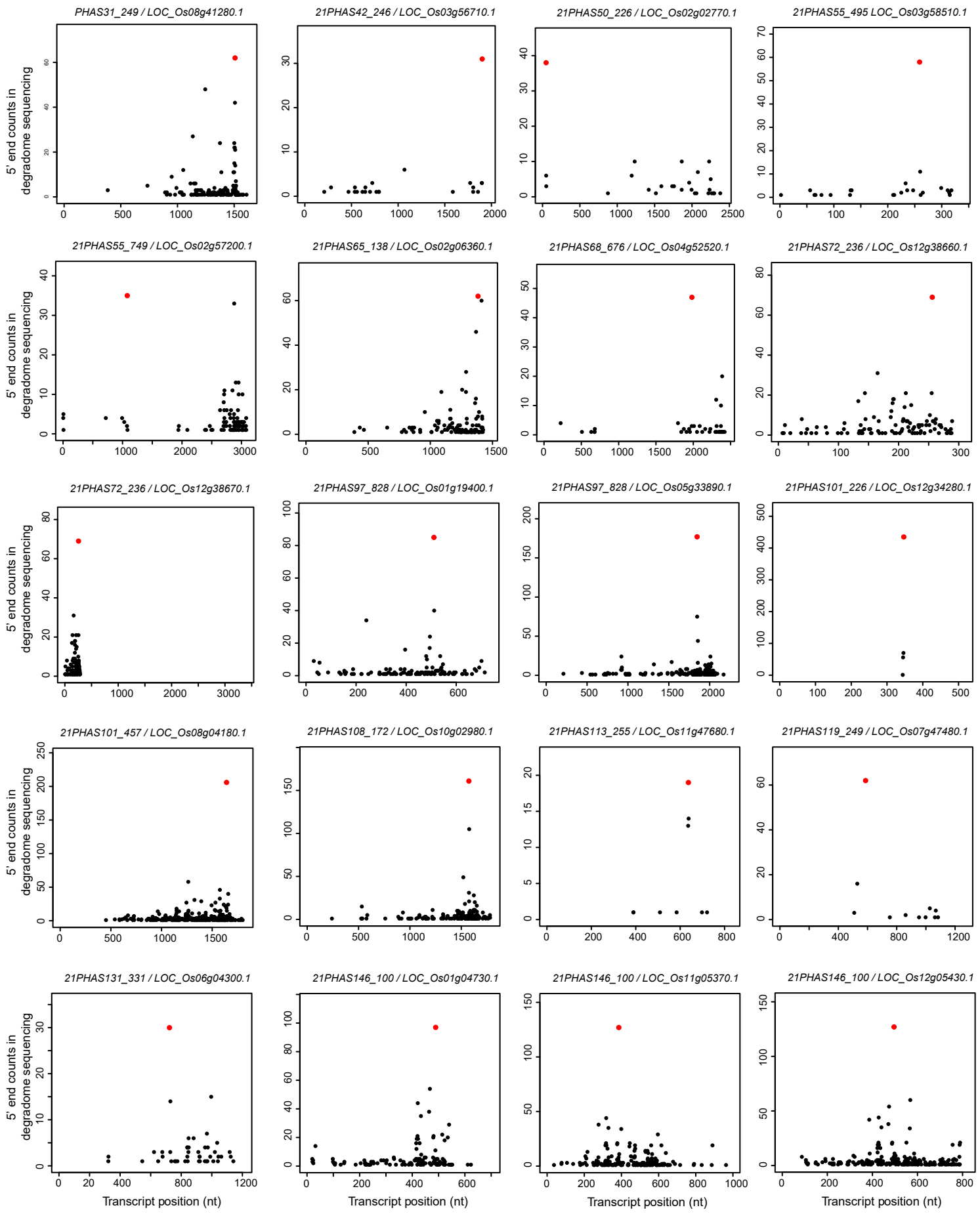


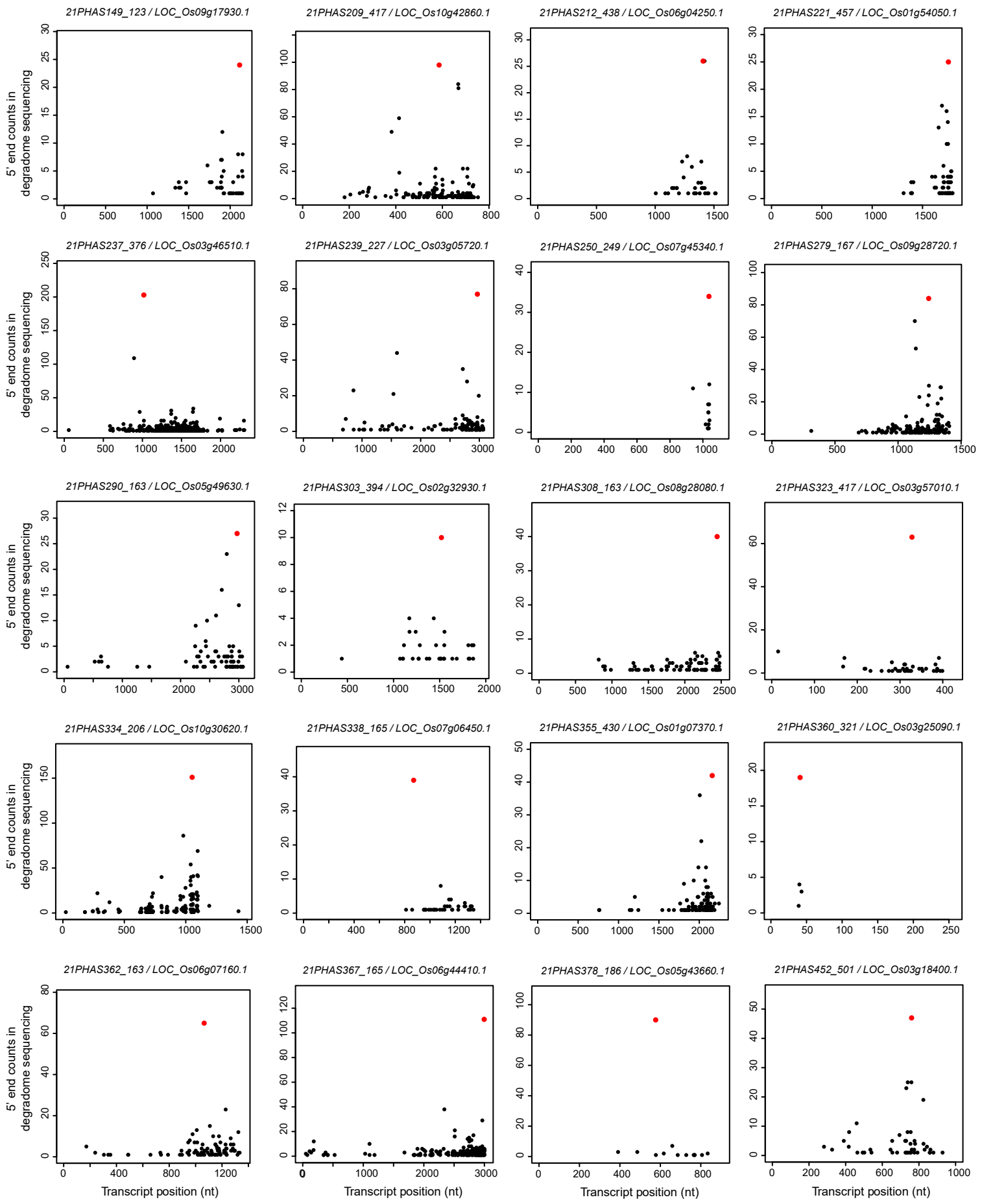


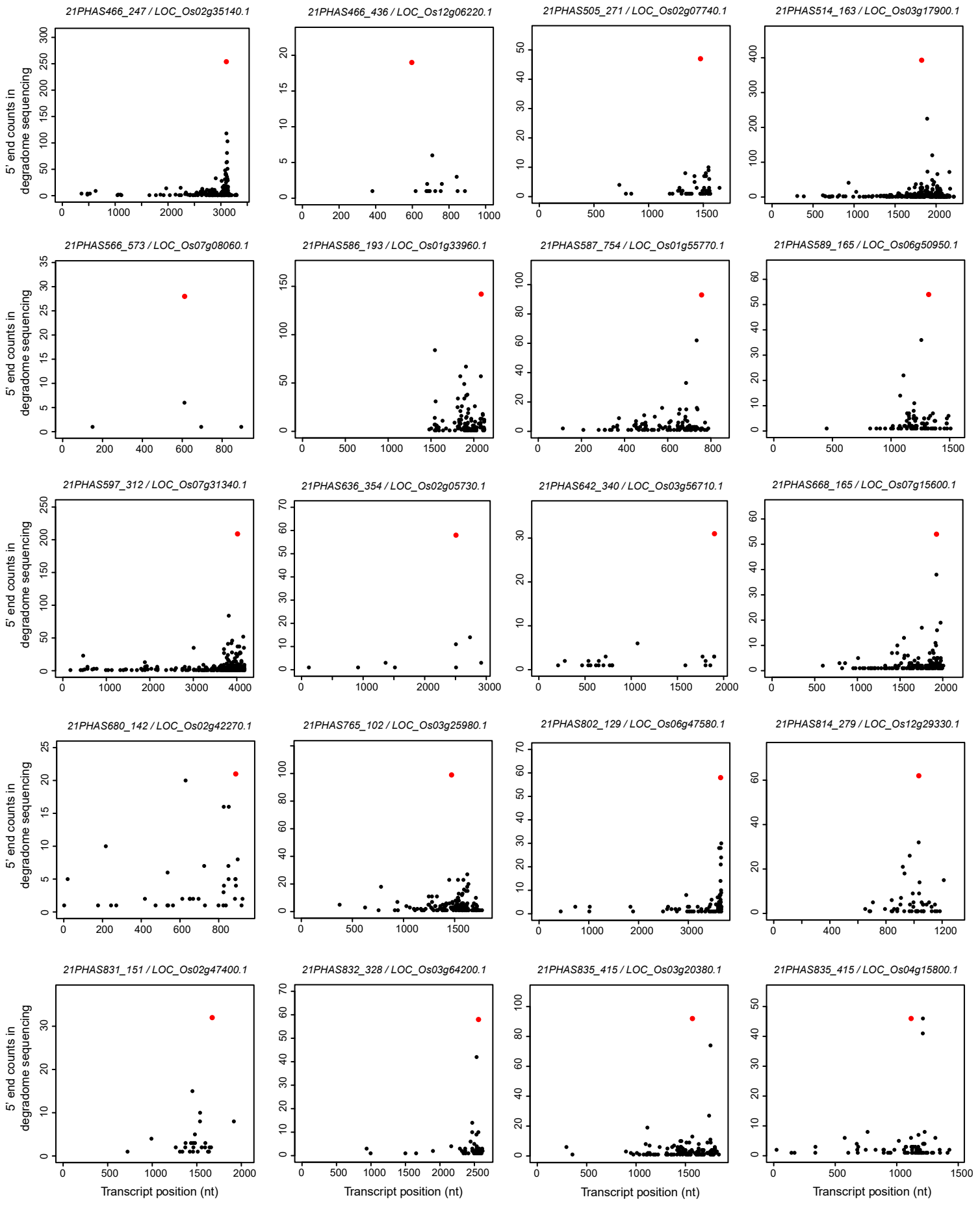


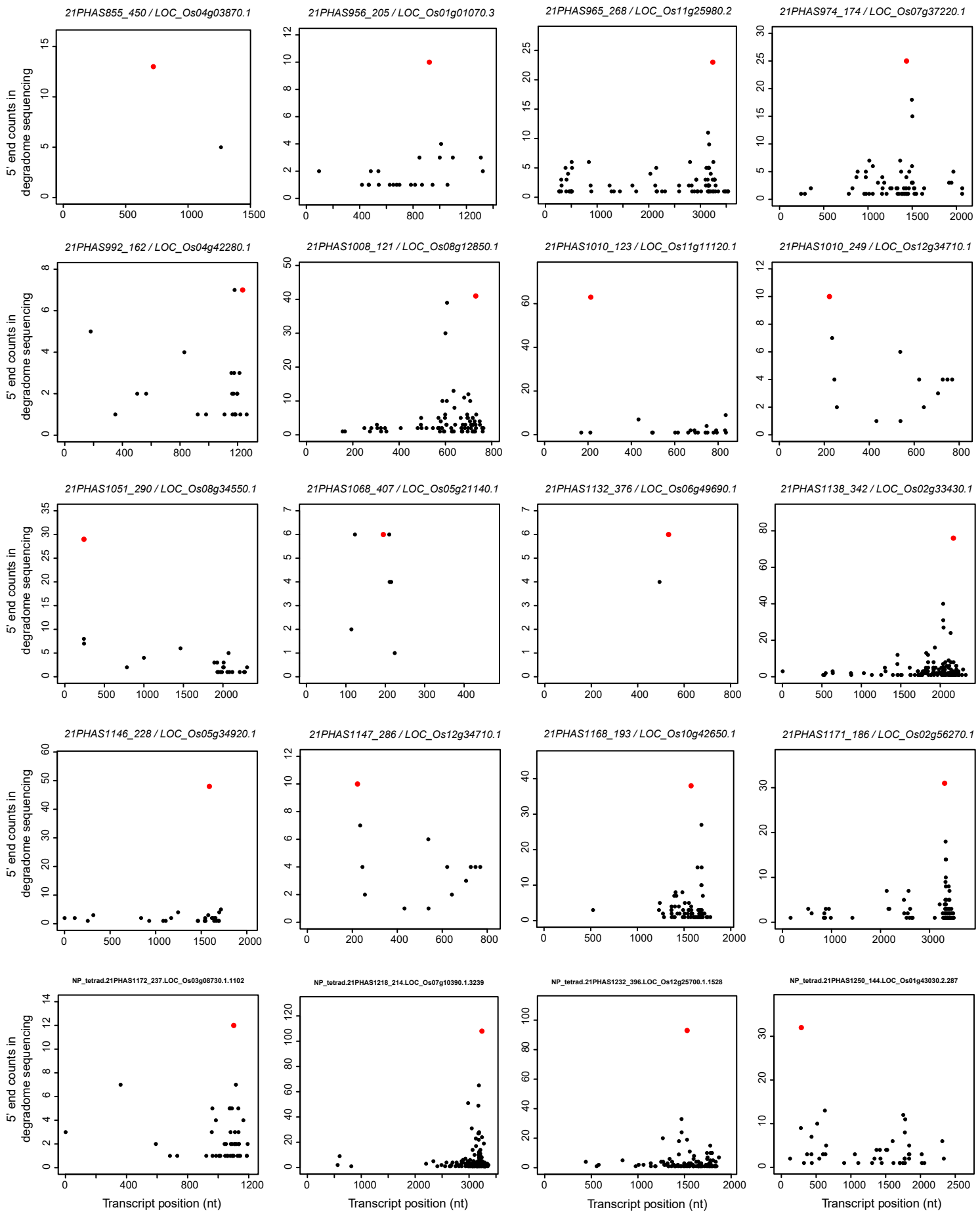


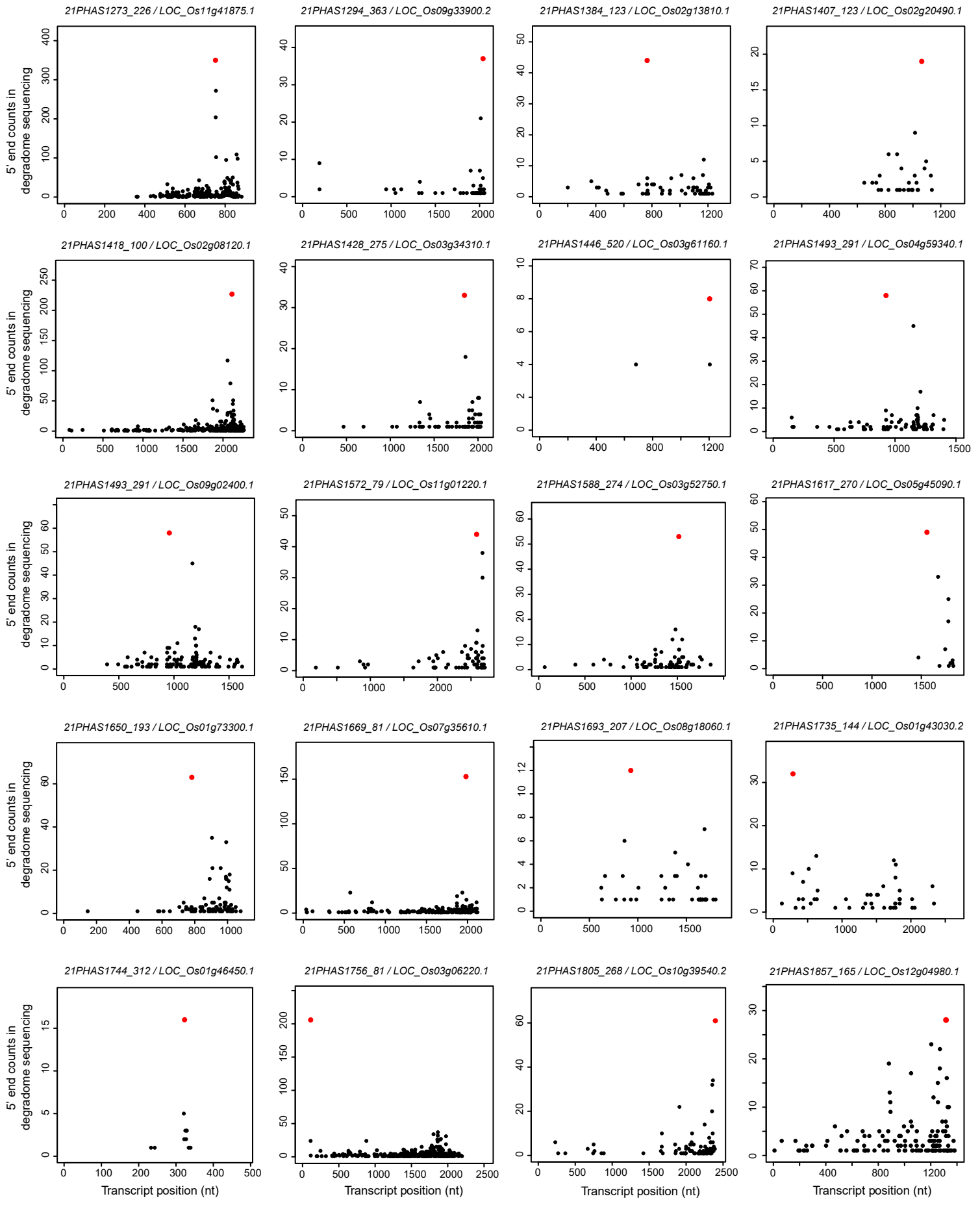
**Supplementary Fig. 6 Validation of 21-nt phasiRNA targets in early prophase I meiocytes by degradome sequencing.** Plots showing the distribution of the degradome tags along 21-nt phasiRNA targets. The x-axis represents the nucleotide position of each target mRNA (5'-3'). The y-axis represents the relative frequency of degradome tags. The red dot represents degradometag at +1 position of 21-nt phasiRNA-guided cleavage site.

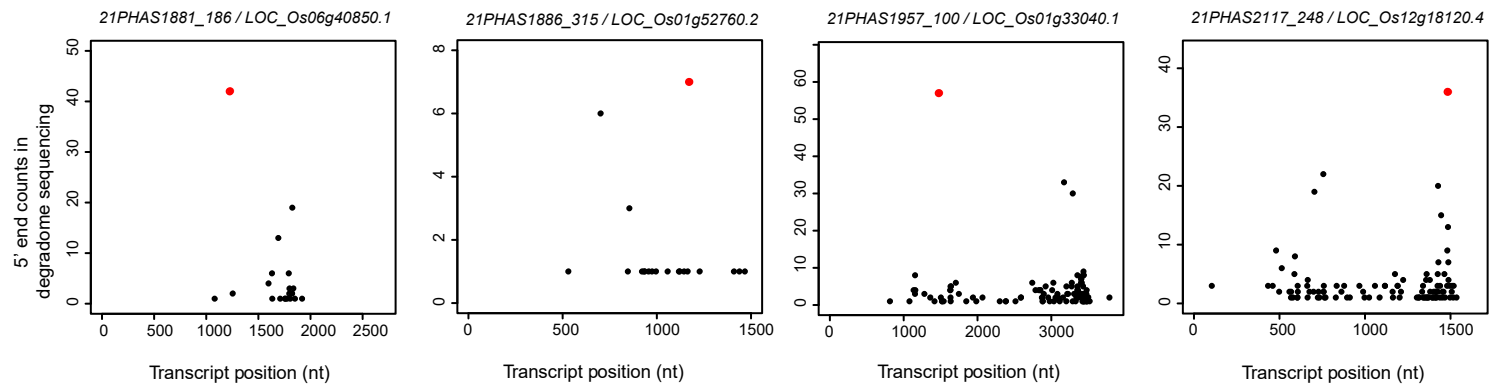






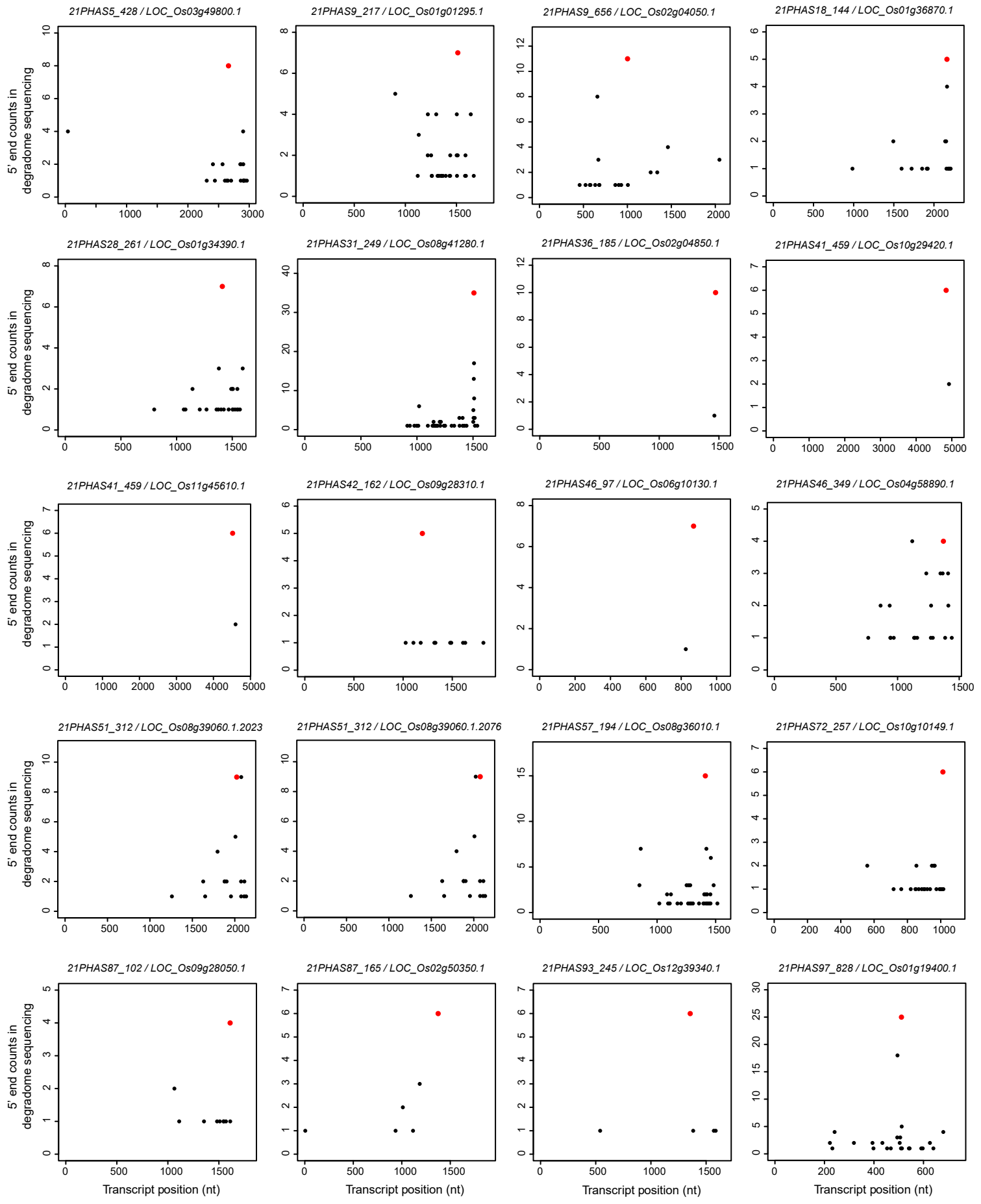


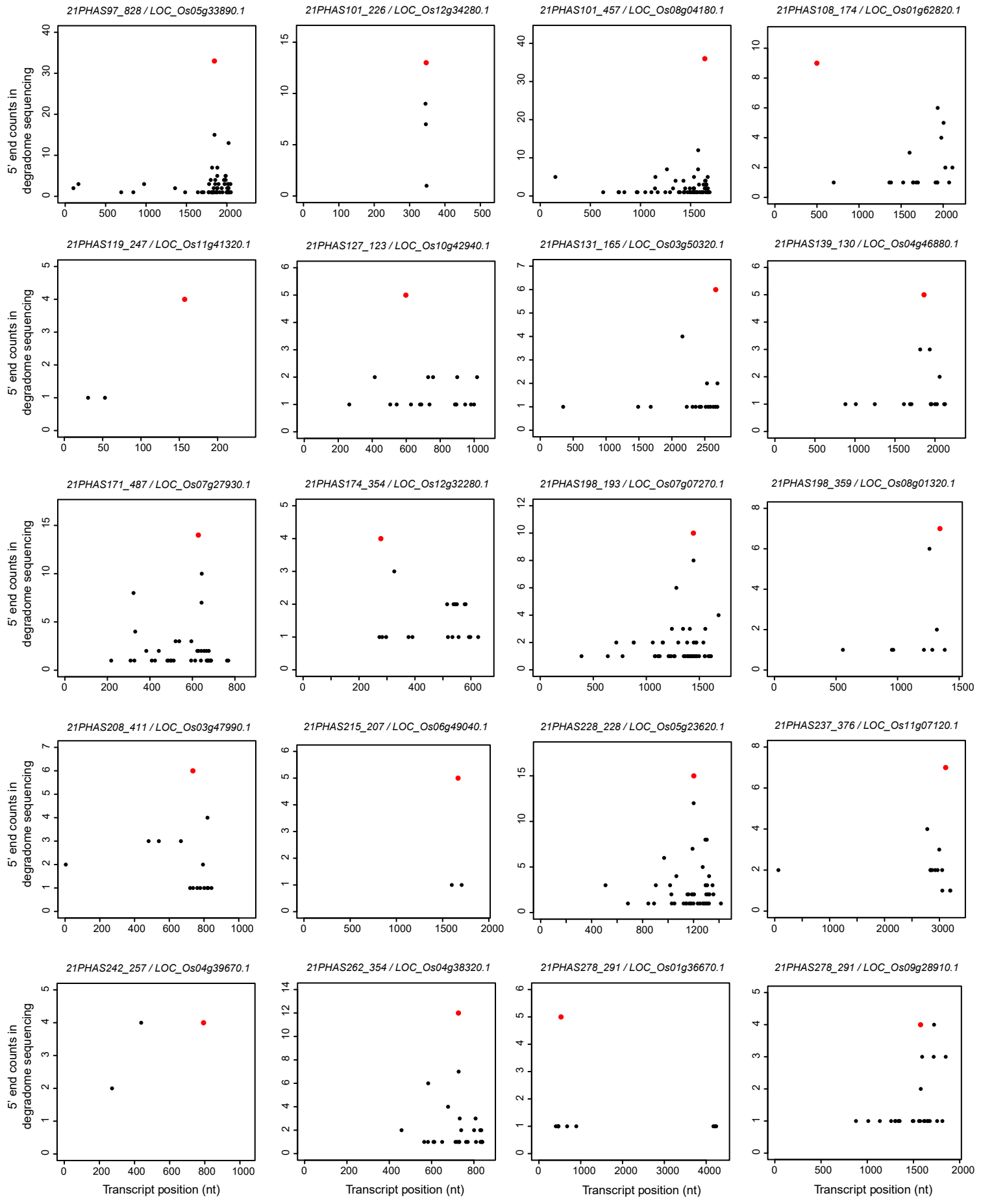


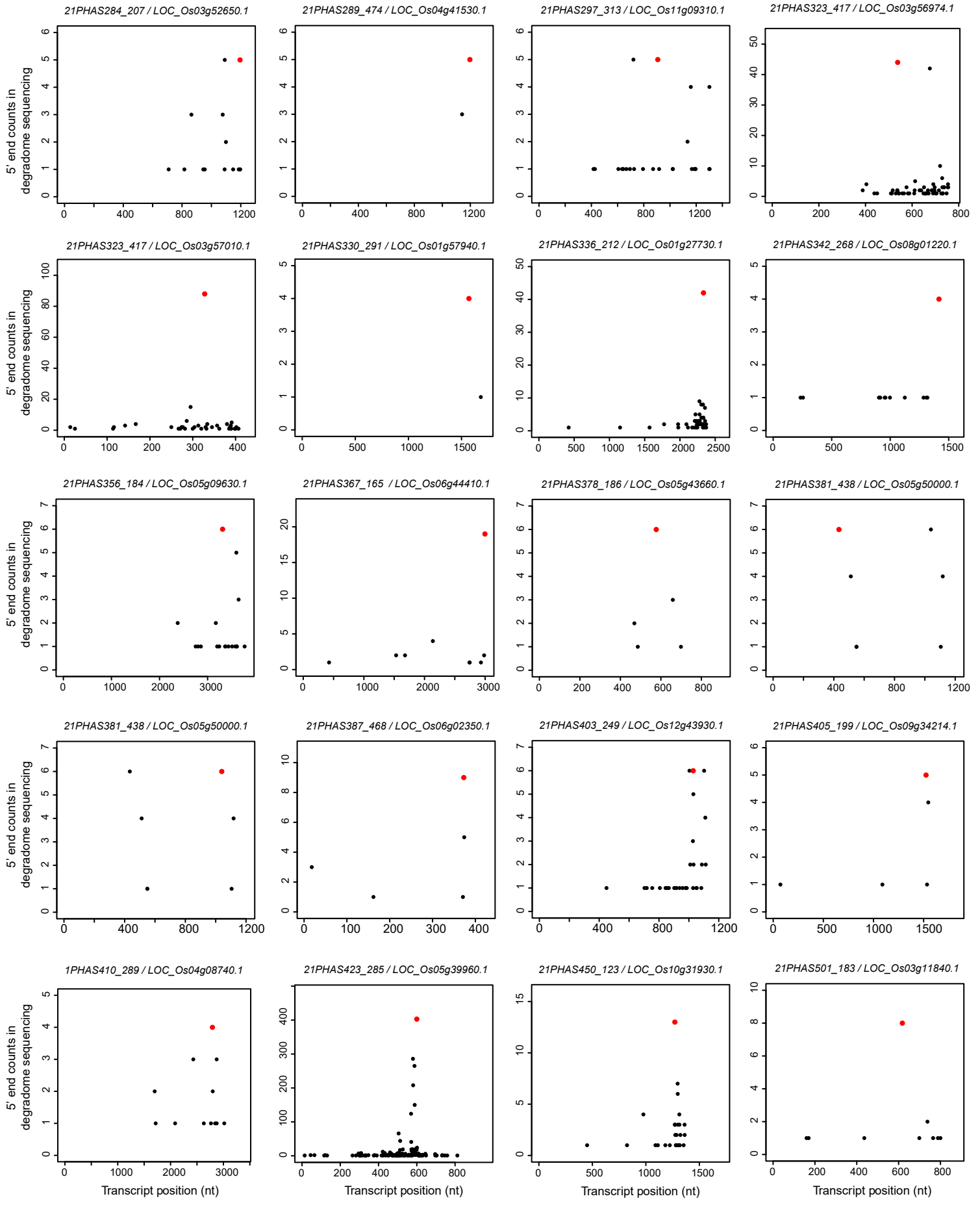


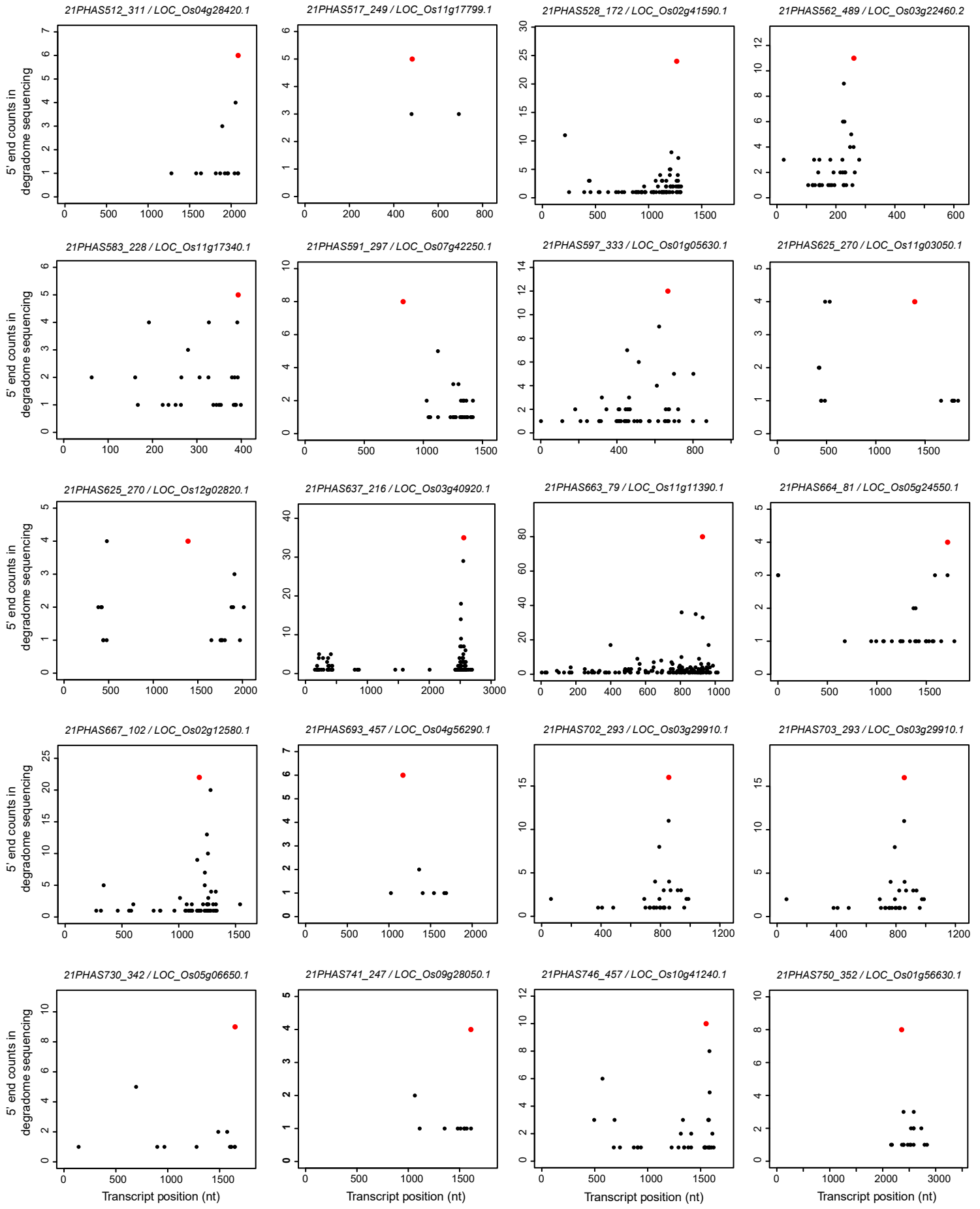
**Supplementary Fig. 7 Validation of 21-nt phasiRNA targets in tetrads by degradome sequencing.**

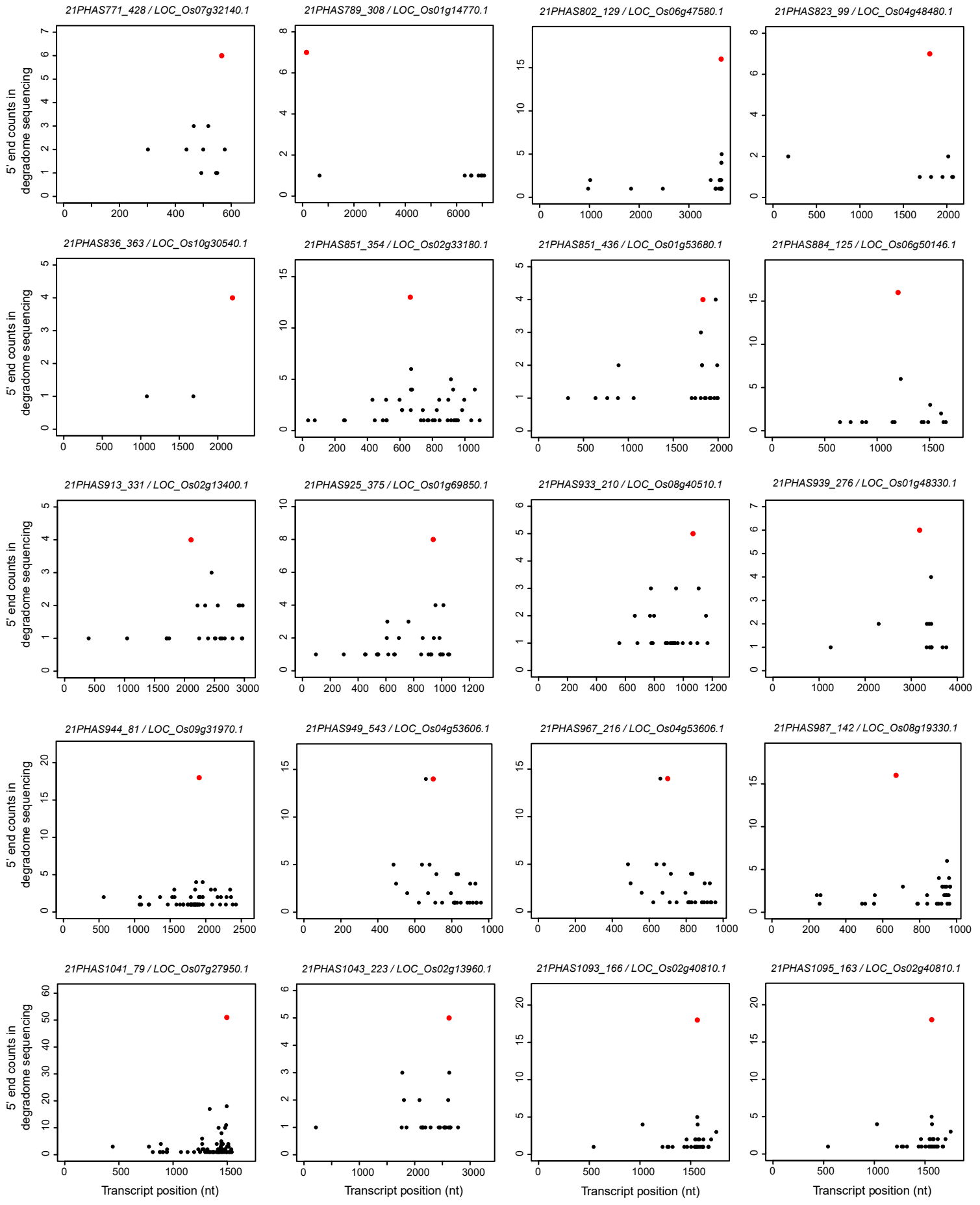
Plots showing the distribution of the degradome tags along 21-nt phasiRNA targets. The x-axis represents the nucleotide position of each target mRNA (5'-3'). The y-axis represents the relative frequency of degradome tags. The red dot represents degradome tag at +1 position of 21-nt phasiRNA-guided cleavage site.

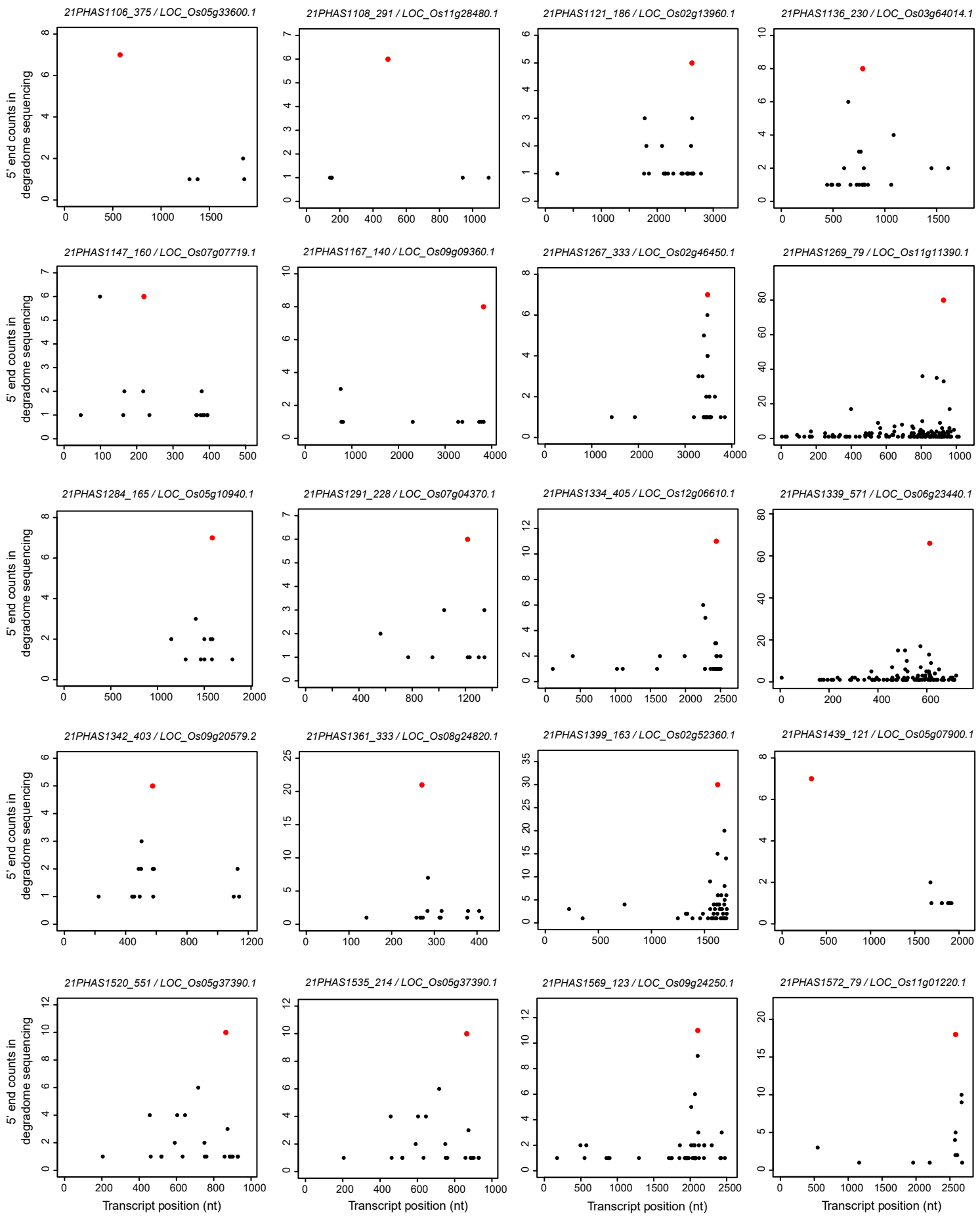


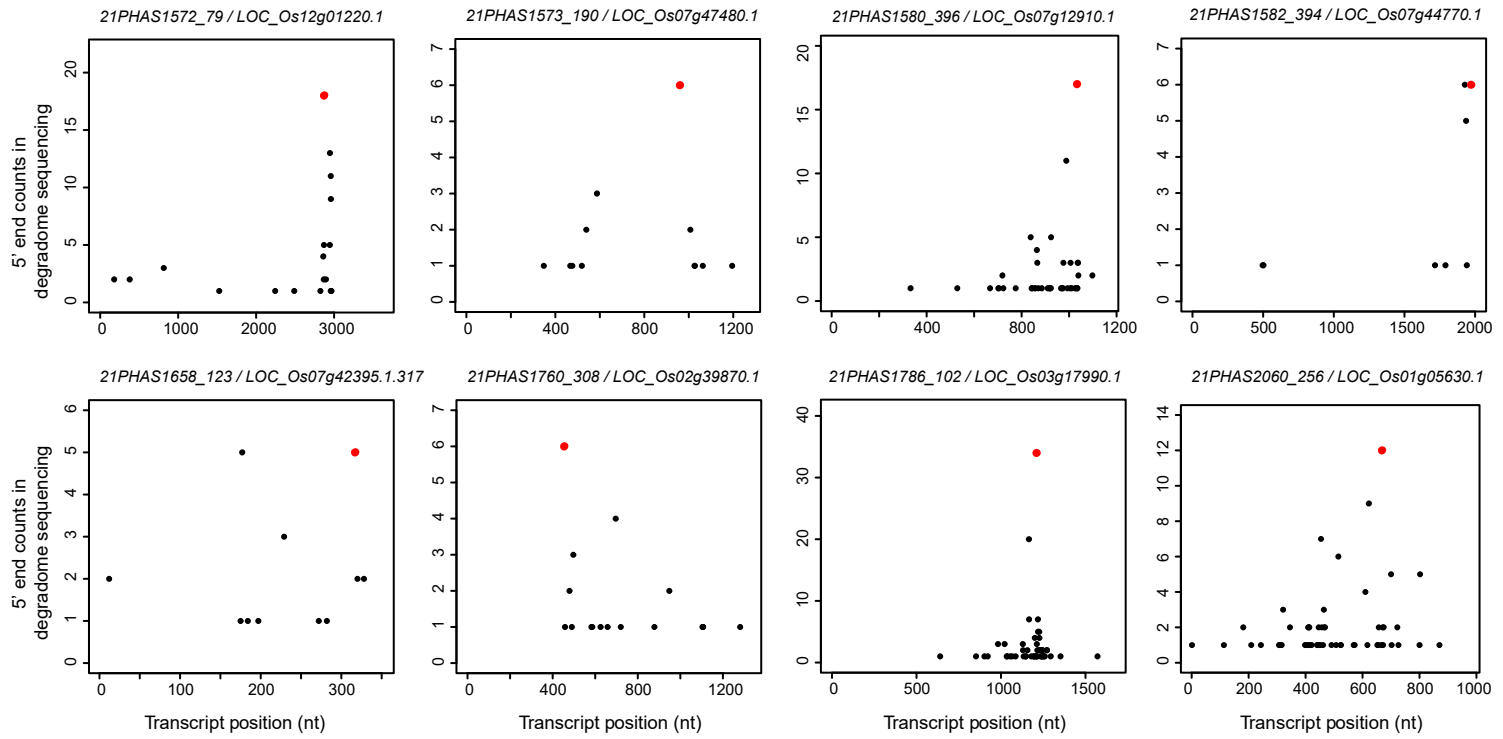




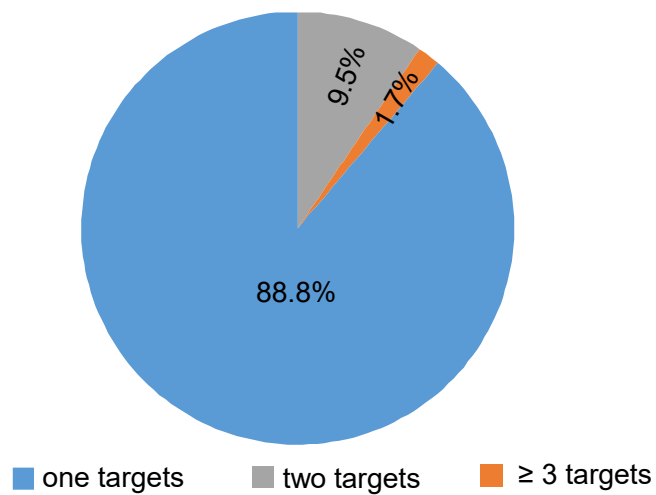




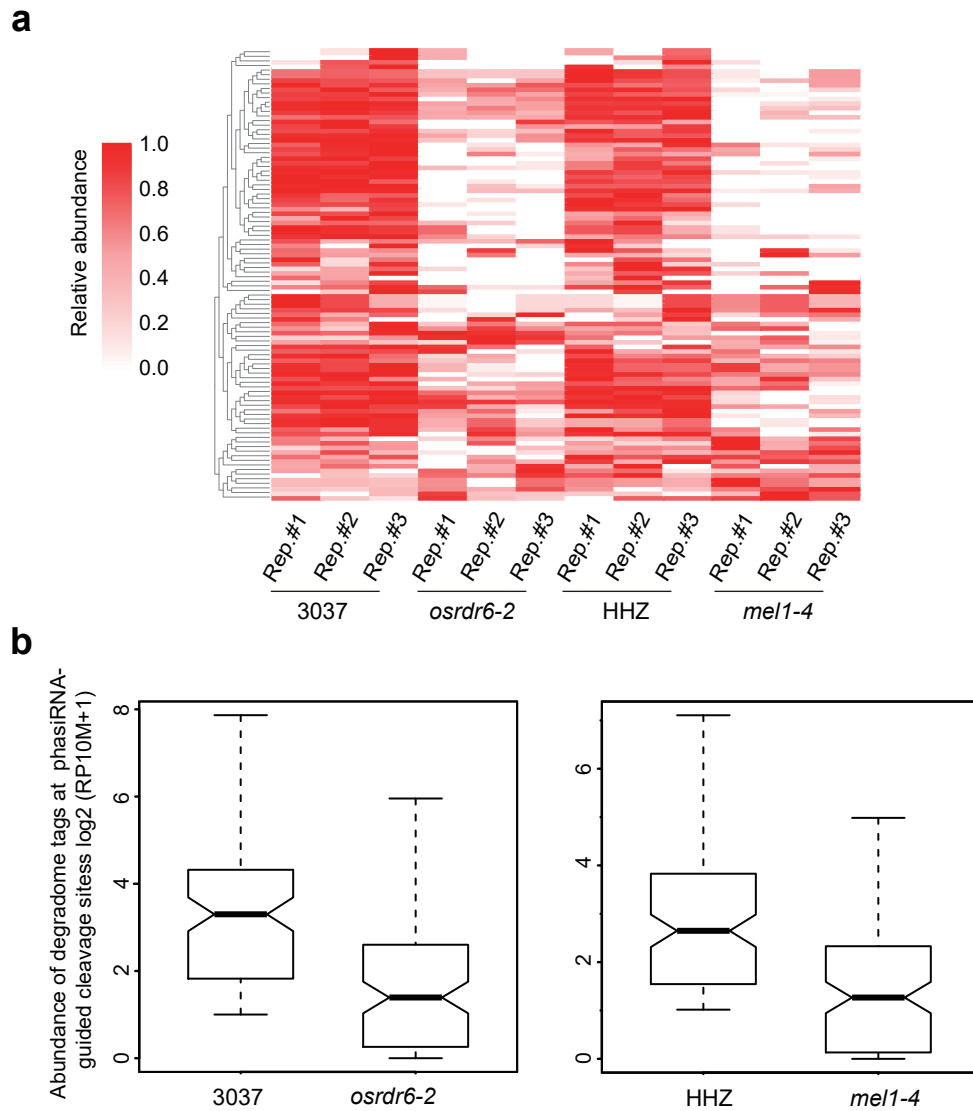




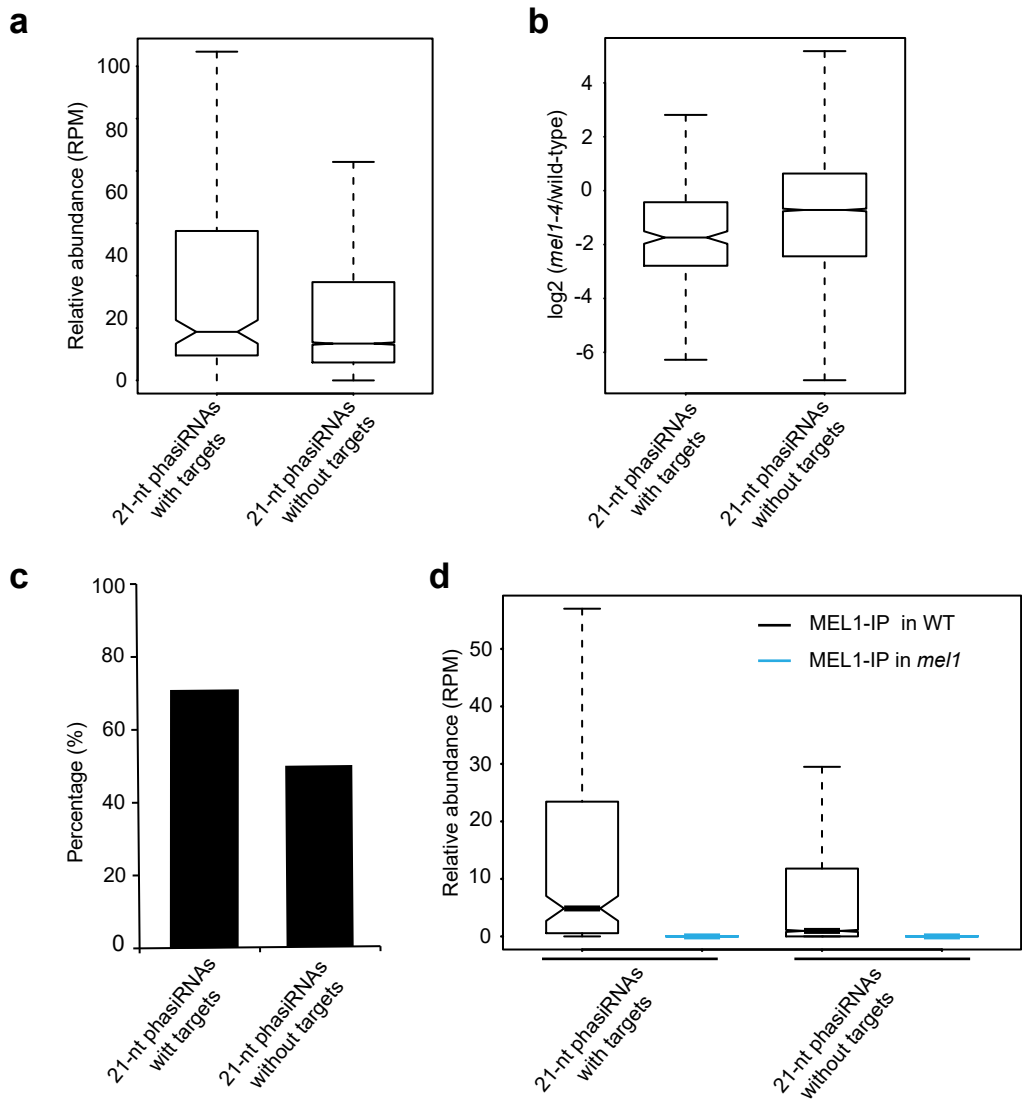
**Supplementary Fig. 8 Validation of 21-nt phasiRNA targets in microspores by degradome sequencing.** Plots showing the distribution of the degradome tags along 21-nt phasiRNA targets. The x-axis represents the nucleotide position of each target mRNA (5'-3'). The y-axis represents the relative frequency of degradome tags. The red dot represents degradome tag at +1 position of 21-nt phasiRNA-guided cleavage site.



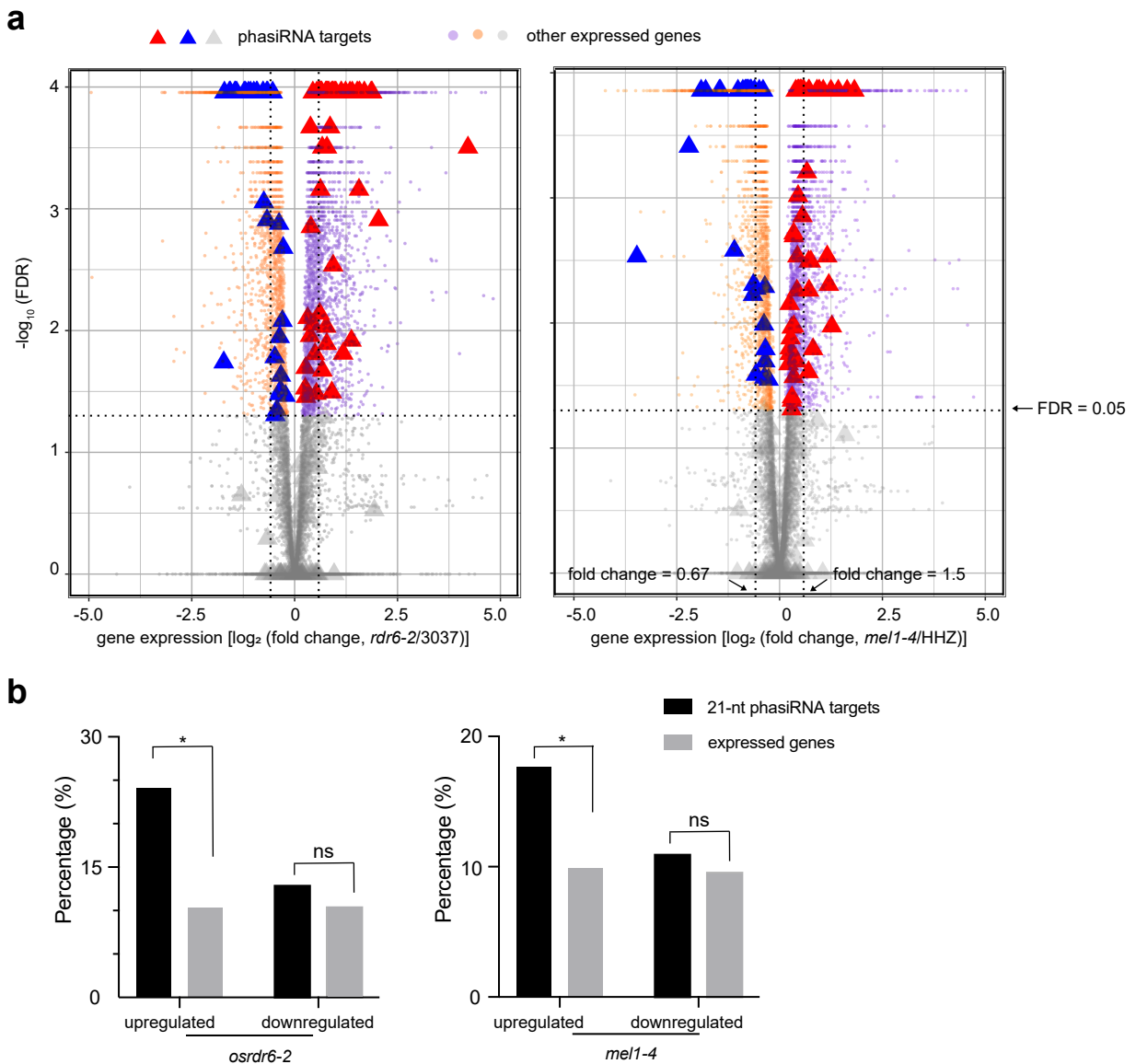
**Supplementary Fig. 9. Analysis of *PHAS* loci with targets.** Pie chart showing the percentages of *PHAS* loci that produce phasiRNAs targeting one, two and three or more genes, respectively.



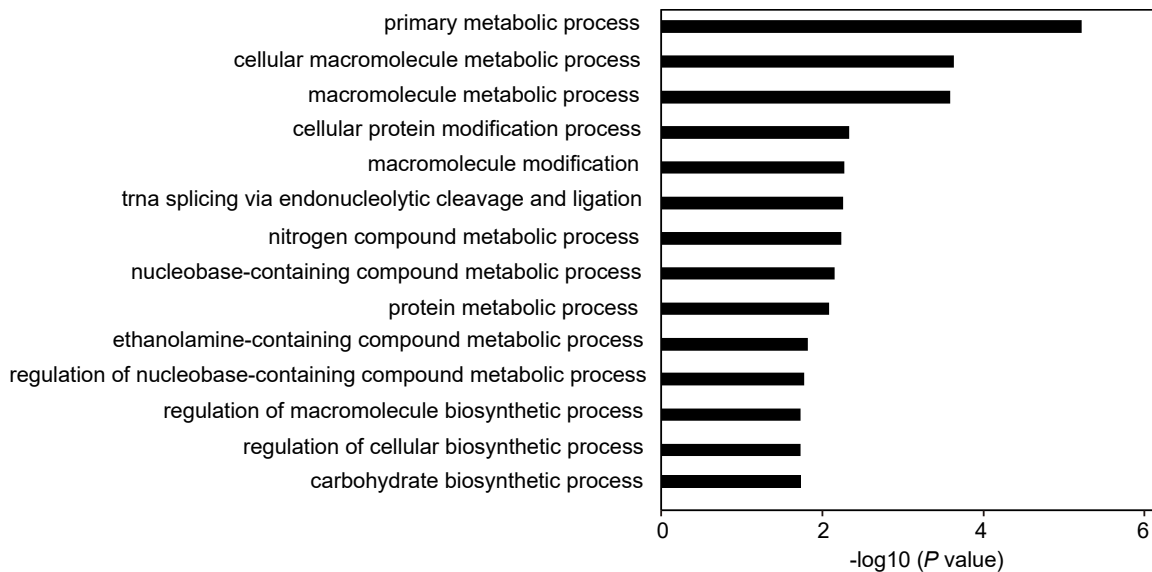
**Supplementary Fig. 10. Relative abundances of degradome tags at phasiRNA-guided cleavage sites in 3037, *osrdr6-2*, HHZ and *mel1-4*.** **a**, Heatmap showing the abundances of degradome tags at +1 positions of 21 -nt phasiRNA-guided cleavage sites in early prophase I meiocytes of *osrdr6-2*, *mel1-4* and their respective wild-type plants. Colors intensity represents the fractional density across the row of log2-transformed (RP10M+1) values. **b**, Box plots showing the log2-transformed (RP10M+1) values in 3037, *osrdr6-2*, HHZ and *mel1-4*. The central line of the box represents the median while two bounds represent 25% quartile and 75% quartile, respectively. The whisker represents  $1.5 \times$  interquartile range of the lower or upper quartile.



**Supplementary Fig. 11. Comparison of the stability of phasiRNAs with and without targets.** **a**, Relative abundances of phasiRNAs with and without cleavage targets in Nipponbare rice plants as determined by sRNA-seq. **b**, Log<sub>2</sub> (fold change) of phasiRNA abundance in *me1-4* relative to its wild-type HHZ. **c**, Percentages of enriched phasiRNAs with and without cleavage targets in MEL1-IP sRNA-seq library. **d**, Relative abundances of phasiRNAs with and without targets in MEL1-IP sRNA-seq library. The central line of the box represents the median while two bounds represent 25% quartile and 75% quartile, respectively. The whisker represents 1.5 × interquartile range of the lower or upper quartile.



**Supplementary Fig. 12. Differential expression of phasiRNA targets in *osrdr6-2* and *mel1-4*.** **a**, Volcano plots showing differential expression of phasiRNA targets and other expressed genes in *osrdr6-2* and *mel1-4*. **b**, Comparison of the percentages of significantly upregulated and downregulated targets in total targets and the percentages of significantly upregulated and downregulated genes in total expressed genes. Fisher's exact test,  $p$ -value  $\leq 0.05$



**Supplementary Fig. 13. Gene ontology enrichment analysis of the 21-nt phasiRNA targets derepressed in early prophase I meiocytes in *osrdr6-2* or *mei1-4*.** GO biological process terms significantly enriched in the targets derepressed in *osrdr6-2* or *mei1-4* are shown. The *P* values were calculated by Fisher's exact test.